JCI The Journal of Clinical Investigation

TNFR2/14-3-3ε signaling complex instructs macrophage plasticity in inflammation and autoimmunity

Wenyu Fu, … , Png Loke, Chuan-ju Liu

J Clin Invest. 2021. https://doi.org/10.1172/JCI144016.

Research In-Press Preview Autoimmunity Inflammation

Graphical abstract

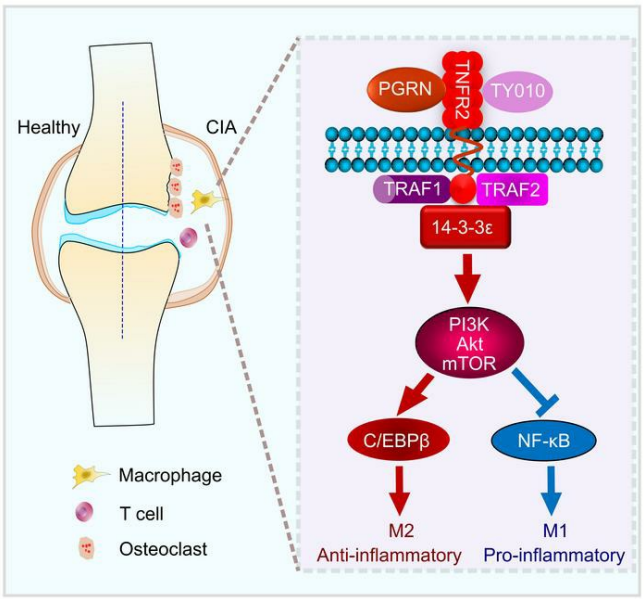

TNFR2/14-3-3ε signaling complex instructs macrophage plasticity in inflammation and autoimmunity

Wenyu Fu[1], Wenhuo Hu[2], Young-Su Yi[1], Aubryanna Hettinghouse[1], Guodong Sun[1], Yufei Bi[1], Wenjun He[1], Lei Zhang[1], Guanmin Gao[1], Jody Liu[1], Kazuhito Toyo-oka[3], Guozhi Xiao[4], David B. Solit[2,5], Png Loke[6], Chuan-ju Liu[1,7]

1. Department of Orthopaedic Surgery, New York University Grossman School of Medicine, New York, New York, USA

2. Human Oncology and Pathogenesis Program, Memorial Sloan Kettering Cancer Center; Marie-Josée and Henry R. Kravis Center for Molecular Oncology, Memorial Sloan Kettering Cancer Center, New York, New York, USA.

3. Department of Neurobiology and Anatomy, Drexel University College of Medicine, Philadelphia, Pennsylvania, USA

4. Department of Biochemistry, School of Medicine, Guangdong Provincial Key Laboratory of Cell Microenvironment and Disease Research, Shenzhen Key Laboratory of Cell Microenvironment, Southern University of Science and Technology, Shenzhen, China

5. Genitourinary Oncology Service, Department of Medicine, Memorial Sloan Kettering Cancer Center, New York, NY 10065, USA

6. Department of Microbiology, New York University Grossman School of Medicine, New York, New York, USA

7. Department of Cell Biology, New York University Grossman School of Medicine, New York, New York, USA

Conflict of interest: The authors have declared that no conflict of interest exists.

Correspondence should be addressed to Dr Chuan-ju Liu, Department of Orthopaedic Surgery, NYU Grossman School of Medicine, 301 East 17th Street, New York NY10003, USA; chuanju.liu@nyulangone.org

Abstract

TNFR1 and TNFR2 have received prominent attention because of their dominance in the pathogenesis of inflammation and autoimmunity. TNFR1 has been extensively studied and primarily mediates inflammation. TNFR2 remains far less studied, although emerging evidence demonstrates that TNFR2 plays an anti-inflammatory and immunoregulatory role in various conditions and diseases. Herein, we report that TNFR2 regulates macrophage polarization, a highly dynamic process controlled by largely unidentified intracellular regulators. Using biochemical co-purification and mass spectrometry approaches, we isolated the signaling molecule 14-3-3ε as a component of TNFR2 complexes in response to progranulin stimulation in macrophages. In addition, 14-3-3ε was essential for TNFR2 signaling-mediated regulation of macrophage polarization and switch. Both global and myeloid-specific deletion of 14-3-3ε resulted in exacerbated inflammatory arthritis and counteracted the protective effects of progranulin-mediated TNFR2 activation against inflammation and autoimmunity. TNFR2/14-3-3ε signaled through PI3K/Akt/mTOR to restrict NF-κB activation while simultaneously stimulating C/EBPβ activation, thereby instructing macrophage plasticity. Collectively, this study identifies 14-3-3ε as a previously-unrecognized vital component of the TNFR2 receptor complex and provides new insights into the TNFR2 signaling, particularly its role in macrophage polarization with therapeutic implications for various inflammatory and autoimmune diseases with activation of the TNFR2/14-3-3ε anti-inflammatory pathway.

Key works: TNFR2, 14-3-3ε, progranulin, macrophage polarization, inflammation, autoimmunity

Introduction

Rheumatoid arthritis (RA) is a common chronic autoimmune condition characterized by inflammatory joint disease (1), resulting from protracted inflammation of the synovial membrane. Macrophages are a major subset of the infiltrating immune cells present in the inflamed joint (2) and are central to the pathophysiology of inflammatory arthritis (3, 4). Functional plasticity is a hallmark of macrophages and phenotypic polarization can occur at any point in the inflammatory process. Disparate phenotypic macrophages play critical, but opposing roles in infectious and autoimmune diseases, inflammatory-associated cancers, and chronic metabolic diseases (5-7). Importantly, macrophage polarization is a highly dynamic process and the phenotype of polarized macrophages can switch under physiological and pathological conditions (8). Although the extracellular signals that induce macrophage phenotypic polarization have been well characterized (9), the intracellular regulators responsible for modulating macrophage polarization and switch are less well known.

TNFα is a pro-inflammatory cytokine that is central to the inflammatory cascade in the pathogenesis of RA (10-12). There are two functionally distinct receptors of TNFα, TNFR1 and TNFR2. TNFR1 primarily mediates inflammatory activity of TNFα, whereas TNFR2 plays a protective and anti-inflammatory role in various diseases and conditions (13-18). Evidence of divergent biologic roles for TNFR1 and TNFR2 in inflammatory arthritis was first reported by Blüml et al. (19), who demonstrated that TNFR1 and TNFR2 deficiencies have distinct and opposing phenotype in a model of erosive arthritis, indicating an anti-inflammatory role of TNFR2. Although TNFR2 signaling was reported to be involved in the function of macrophages (20, 21), TNFR2 signaling is far less well understood relative to TNFR1. In particular, the role of TNFR2 in macrophage plasticity remains unknown.

Progranulin (PGRN) was discovered as a ligand of TNFR2 in our genetic screen and exhibited an approximately 600-fold higher binding affinity to TNFR2 than TNFα (22). Additionally, loss of PGRN

rendered B6 mice highly susceptible to collagen-induced arthritis (CIA), whereas administration of recombinant PGRN prevented the onset and progression of inflammatory arthritis in both TNFα transgenic and CIA models (22-24). Numerous independent laboratories, including ours, have implicated the importance of PGRN/TNFR2 interaction in various kinds of diseases (22, 25-34), including inflammatory arthritis.

In the current study, we take advantage of PGRN's high TNFR2 binding feature to use it as a TNFR2 agonist to activate and delineate TNFR2 signaling. Using biochemical co-purification and mass spectrometry approaches, we isolate the signaling molecule 14-3-3ε as a novel component of TNFR2 complexes in response to PGRN stimulation in macrophages. 14-3-3ε constitutes one of the vital signal molecules recruited by TNFR2 and the TNFR2/14-3-3ε complex supports an anti-inflammatory phenotype in macrophages in inflammatory arthritis. In sum, our work uncovers the molecular mechanisms whereby TNFR2 signaling controls macrophage polarization and demonstrates the potential of targeting this pathway for the treatment of inflammatory and autoimmune disease.

Results

TNFR2 modulates macrophage polarization and switch

To determine whether and how anti-inflammatory and immunoregulatory TNFR2 participated in regulation of macrophage polarization, we first determined the effect of TNFR2 deficiency on bone-marrow-derived macrophages (BMDMs) polarized to M1 and M2 macrophages with LPS/IFNγ and IL-4, respectively (**Figure 1A**). As shown in **Figure 1B**, TNFR2 deletion markedly enhanced the expression of the M1-specific marker genes *Il6* and *Nos2* upon LPS/IFNγ stimulation. In contrast, TNFR2 deletion significantly suppressed the M2-specific marker genes *Arg1* and *Mgl1* upon IL-4 stimulation (**Figure 1C**). Given that macrophage polarization is a dynamic process and macrophages can switch their phenotype as tissue inflammation progresses, we examined whether TNFR2 also regulated the macrophage phenotypic switch *in vitro* (35, 36). More specifically, BMDMs isolated from WT and TNFR2-/- mice were polarized to M1 or M2 macrophages before inducing a phenotypic switch to M2 or M1 macrophages, respectively. Results demonstrated that TNFR2 deletion significantly enhanced the propensity of M2 macrophages to switch into an M1 phenotype but suppressed the phenotypic switch from M1 to M2 (**Figure 1D, E**). In addition, flow cytometry analysis of BMDMs under the polarization conditions revealed a significant enhancement of M1 polarization and reduced M2 polarization in TNFR2-/- BMDMs as compared to WT BMDMs (**Figure 1F, G, and Supplementary Figure 1**). Furthermore, PGRN enhanced M2 and inhibited M1 polarization in WT BMDMs, but these effects were blunted in TNFR2-/- BMDMs (**Figure 1F, G**). It was also noted that PGRN deficiency resulted in phenocopy of TNFR2 deficiency associated alterations in macrophage polarization and phenotypic switch (**Supplementary Figure 2**).

We also compared the effects on macrophage polarization and phenotypic switch by activation of TNFR2 with two different TNFR2 activators: PGRN, known to activate TNFR2 in multiple cell types (22, 25-27, 37), and TY010, a specific TNFR2 agonist antibody (38). As expected, both PGRN and

TY010 dramatically suppressed M1 polarization (**Figure 1B**) and promoted M2 polarization of WT macrophages to a similar extent (**Figure 1C**). Moreover, each activator significantly promoted an M1 to M2 switch and inhibited an M2 to M1 switch in WT macrophages. Notably, these effects on macrophage polarization and phenotypic switch were essentially abolished in macrophages with TNFR2 deletion. In addition, TNFR2 knockdown using siRNA in Raw264.7 macrophages could recapitulate the effects of TNFR2 deficiency in BMDMs in terms of modulating macrophage polarization and switch (**Supplementary Figure 3A-F**).

Besides, TNF neutralizing antibody was used to determine whether PGRN's anti-TNFα/TNFR1 activity contributed to its regulation on M2 polarization. Blockade of TNF activity with anti-TNF antibody did not affect PGRN-promoted M2 macrophage polarization (**Supplementary Figure 4**). Collectively, these results indicated that TNFR2 signaling was crucial for supporting an anti-inflammatory phenotype in macrophages.

14-3-3ε is a component of the TNFR2 complex and required for TNFR2 signaling regulation of macrophage polarization

The finding that the TNFR2 signaling pathway played a pivotal role in controlling macrophage polarization and phenotypic switch led us to hypothesize that activation of TNFR2 by its agonists may recruit different cofactor(s) or adaptors to the receptor complexes, followed by activation of distinct intracellular signaling pathways and downstream gene expression. To isolate such co-factor(s), the intracellular domain (ICD) of TNFR2 was cloned into the PGEX-3X vector to express a fusion of GST to TNFR2ICD. As illustrated in **Figure 2A**, GST (serving as a control) or GST-TNFR2ICD was affinity-purified on glutathione-agarose beads and used as a bait to trap proteins from PGRN-treated Raw264.7 macrophages. These samples were then analyzed by mass spectrometry and MS/MS spectra were searched against the Uniprot database, using Sequest within Proteome Discoverer. After subtracting the hits that were also trapped by the GST column, we found seven proteins specifically

bound to TNFR2 (**Figure 2A**). Identification of TRAF1 and TRAF2, two known TNFR-binding proteins, among the seven hits validated the technique. The highest ranking protein was 14-3-3ε, a regulatory protein belonging to the 14-3-3 family that bound to a wide array of cellular proteins (39, 40). Accumulating evidence suggested that 14-3-3 proteins functioned as "adaptor" or "scaffold" proteins for the assembly of multi-protein signaling complexes (41-44). Thus, 14-3-3ε represented an attractive potential intracellular signaling mediator in the TNFR2 signaling pathway regulating macrophage polarization.

To characterize the role of 14-3-3ε in macrophage polarization, we generated myeloid cell-specific 14-3-3ε deficient mice (**Figure 2B**) (hereafter referred to as 14-3-3ε^{LysM}) by crossing 14-3-3ε$^{f/f}$ mice (45) with LysM-Cre mice (46). 14-3-3ε^{LysM} mice were born in a Mendelian ratio and displayed no overt phenotype. Genomic DNA prepared from tail, T cells, hepatocytes, and macrophages were analyzed by PCR (**Supplementary Figure 5**). Knockout allele was only detectable in the macrophage DNA (**Supplementary Figure 5C**), indicating the Cre recombinase was efficient and specific for macrophages.

LysM-Cre initiated gene deletion within early hematopoietic progenitor cells, concomitant with its activity in neutrophils, which led us to consider whether myeloid-specific 14-3-3ε deficiency influenced macrophage and neutrophil differentiation and proliferation. We first analyzed bone morrow myeloid progenitor subpopulations, including common myeloid progenitors (CMPs), bipotential granulocyte/macrophage progenitors (GMPs), and megakaryocyte/erythrocyte (MEPs) in 14-3-3ε^{LysM} mice vs. controls. 14-3-3ε deficiency neither exhibited apparent effects on CMPs, GMPs and MEPs (**Supplementary Figure 6A-C**), nor perturbed subsequent monocyte/macrophage and neutrophil maturation, as evidenced by undistinguishable frequency of CD11b+F4/80+ and CD11b+Ly6G+ cells in peripheral blood, spleen, and bone marrow (**Supplementary Figure 7A-C**) from that of littermate controls. In addition, loss of 14-3-3ε in myeloid lineage did not affect the proliferation of bone marrow derived macrophages and neutrophils *in vitro* (**Supplementary Figure 7D, E**).

We also generated 14-3-3ε knockout Raw264.7 macrophages using CRISPR-Cas9 technique (**Supplementary Figure 8A, B**). Co-immunoprecipitation with the lysate from control and 14-3-3ε knockout Raw264.7 macrophages, or 14-3-3$\varepsilon^{f/f}$ and 14-3-3ε^{LysM} BMDMs, was performed to confirm the interaction between TNFR2 and 14-3-3ε. As shown in **Figure 2C** and **Supplementary Figure 8C**, TNFR2 was specifically detectable in the immunoprecipitated complex from control macrophages but not 14-3-3ε deficient macrophages, indicating that 14-3-3ε was associated with TNFR2 in macrophages upon stimulation with PGRN. Additionally, immunofluorescence cell staining revealed that 14-3-3ε co-localized with TNFR2 in PGRN-treated Raw264.7 macrophages (**Supplementary Figure 8D**). Taken together, these results indicated that 14-3-3ε was recruited to activated TNFR2 receptor complex in macrophages.

To determine whether other 14-3-3 family members were also differentially regulated in M1 and M2 macrophage, and associated with PGRN or TNFR2, BMDMs isolated from WT, TNFR2-/-, PGRN-/- and 14-3-3ε^{LysM} mice were polarized to M1 or M2. Successful polarization to M1 and M2 macrophages was confirmed by induction of M1 (*Il6*) and M2 (*Arg1*) specific gene expression, respectively (**Supplementary Figure 9A, B**). Using primers specifically designed to detect all 7 isoforms of 14-3-3 family, we found that 14-3-3ε was the only isoform differentially regulated in M1 and M2 macrophages, its expression was down-regulated in M1 and up-regulated in M2 macrophages, and not affected by the deletion of either PGRN or TNFR2 (**Supplementary Figure 9C-I**).

Next, we sought to determine whether 14-3-3ε was important for macrophage polarization and phenotypic switch, BMDMs isolated from 14-3-3$\varepsilon^{f/f}$ and 14-3-3ε^{LysM} mice were first polarized to M1 or M2 macrophages. Gene analysis showed that, as compared to 14-3-3$\varepsilon^{f/f}$ BMDMs, the genes typically linked to M1 macrophages, *Il6* and *Nos2*, were significantly up-regulated in 14-3-3ε^{LysM} BMDMs, whereas *Arg1* and *Mgl1*, associated with the M2 macrophage phenotype, were markedly down-regulated in 14-3-3ε^{LysM} BMDMs. Notably, the effects of TNFR2 activation on macrophage polarization and phenotypic switch were lost in 14-3-3ε^{LysM} BMDMs (**Figure 2D-K**). In addition,

similar results, in terms of enhanced M1 macrophages and M2 to M1 switch, and suppressed M2 macrophages and M1 to M2 switch, were also observed in 14-3-3ε knockout Raw264.7 cells (**Supplementary Figure 10A-D**).

To further characterize the dependence of TNFR2 regulation of macrophage polarization on 14-3-3ε, flag-tagged 14-3-3ε was re-expressed in 14-3-3ε knockout Raw264.7 macrophages (**Figure 3A**). Re-expression of 14-3-3ε in 14-3-3ε knockout Raw264.7 macrophages reversed the phenotype induced by 14-3-3ε deficiency; more importantly, re-expression could restore TNFR2 activation-mediated regulation of macrophage polarization and switch (**Figure 3B-I**). In contrast, over-expression of 14-3-3ε in PGRN knockout Raw264.7 failed to reverse the effects of PGRN deficiency on macrophage regulation (**Supplementary Figure 11A-E**). Collectively, these results indicated that 14-3-3ε was an essential mediator of TNFR2 signaling in controlling macrophage plasticity.

Loss of 14-3-3ε renders mice highly susceptible to collagen-induced arthritis and counteracts TNFR2 activation mediated anti-inflammation

To elucidate the *in vivo* role of TNFR2/14-3-3ε in general inflammation, we generated inducible 14-3-3ε global knockout mice (14-3-3ε-/-) by breeding 14-3-3ε$^{f/f}$ mice with Rosa26a-CreERT2 mice in which Cre-mediated recombination was induced by tamoxifen (47), and then established collagen-induced arthritis (CIA), the most widely-used inflammatory and autoimmune arthritis model, in 14-3-3ε-/- mice and control littermates. Deletion of 14-3-3ε resulted in more severe joint swelling and inflammation as evidenced by significantly higher clinical score, earlier disease onset and greater incidence of arthritis as compared to control mice (**Figure 4A**). Histological and quantitative analysis of whole ankle joints demonstrated 14-3-3ε deletion significantly increased synovitis, osteoclast activity and destruction of bone and cartilage as compared with controls (**Figure 4B, C, and Supplementary Figure 12**). In contrast, injection of TNFR2 agonist PGRN resulted in markedly decreased inflammation, delayed disease onset, reduced incidence of arthritis, and decreased bone and

cartilage destruction in 14-3-3ε$^{f/f}$ mice with CIA (**Figure 4A-C**); more importantly, PGRN's protective effects were mostly abolished in 14-3-3ε-/- mice with CIA (**Figure 4A-C**).

Flow cytometry analyses of the immune cells (**Supplementary Figure 13A, B**) isolated from arthritic joints indicated that neither TNFR2 activation by PGRN nor 14-3-3ε ablation altered macrophage frequency and proliferation (**Figure 4D, E**). However, 14-3-3ε deletion markedly increased mean fluorescence intensity (MFI) of iNos (**Figure 4F**), simultaneous with a decrease of CD206+ (**Figure 4G**) cellsin CD11b+F4/80+ cells, consistent with a strong shift toward M1 macrophages as compared to control. Notably, TNFR2 activation by PGRN significantly decreased MFI of iNos (**Figure 4F**), while CD206+ (**Figure 4G,**) cells increased, and these effects depended on 14-3-3ε, as evidenced by abrogated shift towards to M2 macrophages in PGRN treated 14-3-3ε deficiency mice, and undistinguishable frequency of M1 or M2 macrophages between PBS and PGRN treated 14-3-3ε deficient mice with CIA (**Figure 4F, G**). The number of neutrophils in the joints was comparable between 14-3-3ε$^{f/f}$ and 14-3-3ε-/- mice with CIA, however, PGRN tended to reduce neutrophil populations in a 14-3-3ε independent manner, although the phenomenon did not reach statistical significance. (**Figure 4H**). Neither PGRN nor 14-3-3ε deficiency affected neutrophil proliferation in arthritic joints (**Figure 4I**). Consistently, immunohistochemical staining for myeloperoxidase revealed that neutrophils presented in inflamed joints were undistinguishable between 14-3-3ε$^{f/f}$ and 14-3-3ε-/- CIA mice and PGRN treatment exhibited mild reduction in activated neutrophils in the arthritic joints independent of 14-3-3ε (**Supplementary Figure 14A**).

In support of the notion that CIA induction led to systemic immune response in secondary lymphoid organs including spleen, splenic macrophages displayed similar changes as those observed in arthritic joints; PGRN treatment and 14-3-3ε deletion did not affect the total number of macrophages in the spleen, while PGRN treatment increased M2 and inhibited M1 macrophages in a 14-3-3ε dependent manner (**Supplementary Figures 13C, 15A-C**). We previously reported that PGRN could also affect T cell subtypes in the course of inflammatory arthritis, we thus determined whether these effects also

depended on 14-3-3ε **(Supplementary Figure 13B, D)**. In line with our previous reports that regulation of Tregs contributed to PGRN/TNFR2's anti-inflammation action (22, 26, 37), we found that 14-3-3ε deletion significantly reduced Treg cells in the joints and spleen compared to 14-3-3$\varepsilon^{f/f}$, whereas PGRN treatment markedly enhanced the Treg population compared with PBS treatment in 14-3-3$\varepsilon^{f/f}$ mice with CIA (**Figure 5A, Supplementary Figure 15D**). In addition, PGRN's regulation of Tregs was lost in 14-3-3ε-/- mice (**Figure 5A, Supplementary Figure 15D**). 14-3-3ε deficiency resulted in the increase of IFNγ positive Th1 cells, while PGRN treatment led to reduction of this T cell population, PGRN regulation of Th1 cells was also abolished in 14-3-3ε-/- mice (**Figure 5B, Supplementary Figure 15E**). In contrast, 14-3-3ε deficiency did not affect Th2 and Th17 populations, and PGRN treatment significantly enhanced Th2 and reduced Th17 cells, respectively, in both 14-3-3$\varepsilon^{f/f}$ and 14-3-3ε-/- mice with CIA (**Figure 5C, D, Supplementary Figure 15F, G**), indicating that PGRN's regulation of Th2 and Th17 was 14-3-3ε independent.

We also examined the effects of 14-3-3ε deficiency on the serum levels of cytokines known to be involved in the pathogenesis of inflammatory and autoimmune arthritis. 14-3-3ε deletion boosted serum levels of pro-inflammation cytokines IL-6 and TNFα while suppressed production of anti-inflammation cytokine IL-10 as compared to 14-3-3$\varepsilon^{f/f}$ mice (**Figure 5E-G**). In contrast, PGRN treatment significantly suppressed IL-6, TNFα and IL-1β (**Figure 5E, F, H**) and boosted IL-10 production (**Figure 5G**) in a 14-3-3ε dependent manner. Interestingly, PGRN also suppressed the pro-inflammation cytokine IL-17, independent of 14-3-3ε (**Figure 5I**).

Similar results were observed in PGRN-/- CIA mice compared with WT counterparts. In this case, PGRN deletion also resulted in more severe inflammation, with predominance of pro-inflammatory M1 macrophages (**Supplementary Figure 16A-H**) (22, 26). In addition, PGRN deletion reduced percentages of Tregs, and increased percentages of Th1 and Th17 cells, but had no obvious effect on Th2 cells (**Supplementary Figure 16I-L**).

Collectively, these results suggested that global 14-3-3ε deletion promoted an overt pro-

inflammatory response in CIA, 14-3-3ε deletion could recapitulate the effects of PGRN deletion upon macrophage plasticity, and 14-3-3ε was an essential player in propagation of anti-inflammatory PGRN/TNFR2 signaling in inflammatory and autoimmune arthritis.

Myeloid-specific deletion of 14-3-3ε exacerbates collagen-induced arthritis and abolishes PGRN/TNFR2 regulations of macrophages *in vivo*

To specifically address the role of myeloid-expressed 14-3-3ε in the etiology of inflammation and autoimmunity, and inflammatory and autoimmune arthritis in particular, we also established the CIA model in 14-3-3ε^{LysM} mice. First, we confirmed the efficient deletion of 14-3-3ε in macrophage present in the joints of 14-3-3ε^{LysM} mice with CIA (**Supplementary Figure 17**). Myeloid specific 14-3-3ε deletion resulted in more severe inflammation and earlier disease onset, exacerbated bone and cartilage destruction relative to littermate 14-3-3ε$^{f/f}$ controls (**Figure 6A-C, Supplementary Figure 18**). PGRN was administered to activate TNFR2 signaling in 14-3-3ε^{LysM} mice with CIA in order to determine the importance of myeloid 14-3-3ε for TNFR2 signaling regulation of inflammatory arthritis. PGRN treatment prompted mildly reduced inflammation relative to PBS treatment in 14-3-3ε^{LysM} mice with CIA, although differences did not reach statistical significance. Strikingly, PGRN's suppression of inflammation in 14-3-3ε^{LysM} mice was largely abolished relative to littermate 14-3-3ε$^{f/f}$ controls (**Figure 6A-C**). In addition, 14-3-3ε^{LysM} mice had increased number of osteoclasts relative to their littermate controls, whereas PGRN inhibited osteoclast number in a 14-3-3ε dependent manner (**Supplementary Figure 18C, D**). To investigate whether 14-3-3ε deficiency affected osteoclastogenesis *in vitro*, osteoclast differentiation was induced using BMDMs isolated from WT and 14-3-3ε^{LysM} mice. 14-3-3ε deficiency did not affect RANKL-induced osteoclastogenesis, but enhanced TNFα and RANKL co-stimulated osteoclastogenesis. Additionally, PGRN inhibited TNFα enhanced osteoclastogenesis which relied on 14-3-3ε (**Supplementary Figure 19A, B**). These results suggested that increased osteoclasts seen in 14-3-3ε^{LysM} mice with CIA might also be attributed to disturbed osteoclastogenesis, apart from

the elevated inflammation which is known to promote osteoclastogenesis (48, 49).

Flow cytometry analysis revealed that total number and proliferation of macrophage infiltrated in inflamed joints were unchanged in 14-3-3ε^{LysM} mice relative to littermate 14-3-3ε$^{f/f}$ controls (**Figure 6D, E**). Despite unchanged macrophage accumulation and proliferation in the arthritic joints, 14-3-3ε^{LysM} mice exhibited higher MFI of iNos, and lower CD206+ cells in CD11b+F4/80+ cells relative to littermate 14-3-3ε$^{f/f}$ controls (**Figure 6F, G**), closely recapitulating the characteristic macrophage phenotype of 14-3-3ε-/- mice. Again, in a similar manner as seen in 14-3-3ε-/- mice, PGRN treatment skewed macrophages towards the M2 phenotype in 14-3-3ε$^{f/f}$ controls while this effect was lost in 14-3-3ε^{LysM} mice. Additionally, both recombinant PGRN and 14-3-3ε deficiency did not exert significant effects on number and proliferation of infiltrating neutrophils in the joints of the CIA mice (**Figure 6H, I, Supplementary 14B)**. As expected, myeloid specific deletion of 14-3-3ε did not affect the T cell subtypes in the arthritic joints (**Figure 7A-D**). Moreover, the phenotype of immune cells in spleen could closely recapitulate those in inflamed joints (**Supplementary Figure 20A-G**). Analysis of serum cytokine levels demonstrated that IL-6 and TNFα (**Figure 7E, F**) were the major pro-inflammation cytokines impacted by myeloid sourced 14-3-3ε given that all other cytokines measured (IL-1β, IL-17, and IL-10) were comparable between 14-3-3ε$^{f/f}$ and 14-3-3ε^{LysM} CIA mice (**Figure 7G-I**). PGRN's regulation of IL-6 and TNFα depended on macrophage 14-3-3ε, as evidenced by loss of these effects in 14-3-3ε^{LysM} CIA mice; however, PGRN's regulations of IL-1β, IL-17, and IL-10 production were independent of myeloid 14-3-3ε (**Figure 7E-I**). Together, these results indicated that myeloid-expressed 14-3-3ε played an important role in TNFR2 signaling mediated regulation of macrophages and anti-inflammatory activity in inflammatory and autoimmune arthritis.

14-3-3ε deficiency leads to the alterations of the intracellular signaling in macrophages

To elucidate the molecular mechanisms by which 14-3-3ε regulated macrophage plasticity, we performed unbiased RNA-seq on BMDMs isolated from 14-3-3ε$^{f/f}$ and 14-3-3ε^{LysM} mice stimulated

with pro-inflammatory LPS/IFNγ or anti-inflammatory IL-4. 815 genes (396 down-regulated and 419 up-regulated) were differentially expressed (fold change > 2, FDR < 0.05) in LPS-treated 14-3-3ε^{LysM} BMDMs compared with 14-3-3ε$^{f/f}$ BMDMs (**Figure 8A, Supplementary Table 1**), and 583 genes (291 down-regulated and 292 up-regulated) were differentially expressed (fold change > 2, FDR < 0.05) in IL-4-treated 14-3-3ε^{LysM} BMDMs compared with 14-3-3ε$^{f/f}$ BMDMs (**Figure 8B, Supplementary Table 2**). Similarly, PGRN deficiency was associated with an altered transcriptome pattern (**Supplementary Figure 21A, B**). Gene set enrichment analysis (GSEA) revealed that both 14-3-3ε deficiency and PGRN deficiency altered gene expression patterns in macrophages. Specifically, genes associated with inflammation such as interferon gamma response, interferon alpha response, and inflammatory response were largely upregulated in 14-3-3ε^{LysM} and PGRN-/- BMDMs compared with WT BMDMs (**Figure 8C, Supplementary Figure 21C, 22A-C**). Intriguingly, GSEA analysis indicated that TNFα/NF-κB and PI3K/Akt/mTOR signaling pathways were impaired in both 14-3-3ε deficient and PGRN deficient macrophages (**Figure 8C, Supplementary Figure 22D, E**) compared with WT BMDMs, suggesting that TNFα signaling and PI3K signaling might be the key pathways regulated by the TNFR2/14-3-3ε complex in macrophage polarization. In addition, it was previously reported that PGRN activated Akt signaling and inhibited TNFα signaling in various kinds of cells (50). Further, increasing evidence demonstrated that activation of the PI3K/Akt pathway was critical in restricting pro-inflammatory and promoting anti-inflammatory response in macrophages (51-56). GSEA analysis, together with these aforementioned reports, led us to examine whether PI3K/Akt/mTOR and TNFα signaling were involved in TNFR2/14-3-3ε's regulation of macrophage polarization. Firstly, we examined the effect of PGRN on LPS-stimulated Akt phosphorylation and found that PGRN activated Akt phosphorylation in macrophages (**Figure 8D, E**). In contrast, inhibition of PI3K or mTOR by their specific inhibitors was sufficient to enhance M1 macrophages and inhibit M2 macrophages, and block PGRN's effects on macrophage polarization (**Figure 8F**). Furthermore, both 14-3-3ε deficiency and PGRN deficiency inhibited LPS-stimulated Akt phosphorylation (**Figure 8G, H, Supplementary**

Figure 23A). In brief, PI3K/Akt/mTOR signaling was important for TNFR2/14-3-3ε signaling in regulating macrophage polarization.

TNFR2/14-3-3ε signaling inhibits NF-κB activation and stimulates C/EBPβ activation during macrophage polarization

GSEA analysis indicated that genes associated with inflammation, such as interferon response and inflammatory response, were largely up-regulated in 14-3-3ε deficient BMDMs compared with WT BMDMs. To further identify the transcription factor(s) that modulated enhanced inflammation in 14-3-3ε deficient BMDMs, we searched for targets of these pathways using TFactS (57) and identified NF-κB1 (p105) and Rela (NF-κB p65) as significantly activated transcription factors and C/EBPβ as a significantly inhibited transcription factor in 14-3-3ε deficient BMDMs (**Figure 9A**) that could modulate these inflammatory signaling pathways. The PI3K/Akt/mTOR signaling pathway was reported to act as a negative regulator of NF-κB signaling, leading to inhibited M1 macrophage response (54, 58, 59), but has also been linked to activation of transcription factor C/EBPβ, in turn promoting M2 macrophage response (54, 60). In line with the TFactS assay and previous reports, 14-3-3ε deficiency inhibited IL-4-stimulated C/EBPβ phosphorylation (**Figure 9B, C**) and inhibited LPS-induced Akt phosphorylation while simultaneously enhanced LPS-induced phosphorylation of IκKα/β and NF-κB p65 (**Figure 9D, E**). Given that NF-κB p65 promoted the expression of pro-inflammatory cytokines (61, 62), whereas C/EBPβ promoted the expression of anti-inflammatory cytokines in macrophages (60, 63, 64), we assessed the DNA binding activity of NF-κB p65 and C/EBPβ in macrophages in the presence or absence of 14-3-3ε. 14-3-3ε deficiency rapidly and sustainably enhanced LPS-stimulated p65 DNA binding activity as compared to WT macrophage (**Figure 9F**), whereas the opposite was seen for IL-4-induced C/EBPβ DNA binding activity (**Figure 9G**). These results indicated that 14-3-3ε acted as the suppressor of LPS/ NF-κB signaling in M1 macrophage polarization and the activator of IL-4/ C/EBPβ signaling in M2 macrophage polarization. In addition,

PGRN deficiency also led to the inhibition of LPS-stimulated Akt phosphorylation and enhancement of LPS-stimulated phosphorylation of IκKα/β and NF-κB p65 (**Supplementary Figure 23A, B**), whereas IL-4-stimulated C/EBPβ phosphorylation was inhibited (**Supplementary Figure 23C, D**). Further, analogous to observations in 14-3-3ε deficient macrophages, PGRN deficiency enhanced LPS-stimulated NF-κB p65 DNA binding (**Supplementary Figure 23E**) and suppressed IL-4-induced C/EBPβ DNA binding activity (**Supplementary Figure 23F**). Collectively, these mechanistic findings with 14-3-3ε deficient and PGRN deficient macrophages further implicated the importance of 14-3-3ε in PGRN/TNFR2 regulation of macrophage polarization.

Discussion

Inflammatory and autoimmune arthritis is a polyarticular chronic inflammatory disease characterized by deregulated immune response and bone erosion. Increasing evidence documents that macrophages significantly contribute to inflammation in inflammatory arthritis (5, 65), thus therapeutic strategies targeting the unbalanced M1/M2 ratio represent an attractive goal in treating inflammatory and autoimmune arthritis. Although it is well recognized that TNFR2 plays a beneficial anti-inflammation function in inflammatory and autoimmune diseases, its role in macrophage polarization remains a poorly understood facet. Here, we found that TNFR2 played a critical role in regulating phenotypic polarization in macrophages. Activation of TNFR2 with its ligand PGRN markedly skewed the macrophage toward anti-inflammatory M2 macrophages. Interestingly, in support of TNFR2 activation as a critical regulator of macrophage polarization, TY010, the specific TNFR2 agonist antibody (38), largely recapitulated the effects of PGRN on macrophage polarization. More importantly, using biochemical co-purification and mass spectrometry approaches, we isolated the signaling molecule 14-3-3ε as a pivotal component of TNFR2 complexes in response to PGRN stimulation and a key participant of PGRN/TNFR2 signaling mediated management of macrophage polarization, without affecting macrophage migration or proliferation.

14-3-3ε is a regulatory protein of the 14-3-3 family which binds to a wide array of cellular proteins [37, 38] and can function as “adaptor” or “scaffold” proteins for the assembly of multi-protein signaling complex [39-42].14-3-3ε deficiency in macrophages resulted in an overt pro-inflammatory response through skewing macrophages toward M1 phenotype *in vitro*. In addition, genetic 14-3-3ε deletion resulted in severe inflammation and unbalanced M1/M2 ratio relative to WT littermate controls, which suggested that unbalanced M1/M2 ratio played a pathologic role in inflammatory and autoimmune arthritis, and targeting macrophage plasticity through 14-3-3ε may hold therapeutic value. This study specifically focused on the role of intracellular 14-3-3ε, which was recruited to the TNFR2

intracellular domain following activation by TNFR2 ligand/agonist to mediate signaling through the TNFR2 pathway in macrophages. However, it has also been reported that extracellular 14-3-3ε could regulate chondrocyte metabolism (66). Whether and how extracellular 14-3-3ε regulates macrophage polarization, as well as functional comparisons of intracellular and extracellular 14-3-3ε in other cell types present in joints, including chondrocytes and osteocytes, warrants further investigations.

Several labs, including ours, have shown that the anti-inflammatory activities of PGRN depended largely on TNFR2 (22, 25, 26, 31, 67). In current study, we successfully characterized 14-3-3ε as a component of TNFR2 complexes in macrophages. Our *in vitro* studies demonstrated that PGRN-/-, TNFR2-/- and 14-3-3ε-/- macrophages exhibited enhanced M1 and reduced M2 polarization to comparable extent, while recombinant PGRN exerted opposite effects on macrophage polarization and these effects depended on TNFR2 and 14-3-3ε. Strikingly, the finding that re-expression of 14-3-3ε restored 14-3-3ε knockout cells' response to PGRN, while its over-expression failed to reverse PGRN deficiency's effects on macrophage polarization, indicated that 14-3-3ε served as an essential mediator of PGRN/TNFR2 signaling. Several findings, including enhanced susceptibility to murine CIA following global deletion of 14-3-3ε, recapitulation of global 14-3-3ε deletion's effects on macrophage plasticity following myeloid-specific deletion of 14-3-3ε, and blockade of PGRN's anti-inflammation action in 14-3-3ε deficient CIA mice, provided genetic evidence demonstrating that 14-3-3ε was a crucial co-factor of TNFR2 and engaged in mediating TNFR2 signal's anti-inflammatory phenotype. Furthermore, our data indicated IL-6 and TNFα were two major pro-inflammatory cytokines secreted and regulated by macrophages via the TNFR2/14-3-3ε signaling pathway; the importance of IL-6 and TNFα in mediating pro-inflammatory response and bone erosion had been highlighted by numerous experimental and clinical observations (4, 12, 68-70).

One limitation of using LysM-Cre to determine the role of PGRN/TNFR2/14-3-3ε in modulating macrophage plasticity during CIA was that LysM-Cre mediated deletion of 14-3-3ε in neutrophils may also impact PGRN/TNFR2 regulation of inflammation in CIA. Neutrophil analyses with both 14-3-3ε-

/- and 14-3-3ε^{LysM} revealed that 14-3-3ε deletion did not affect neutrophil infiltration in inflamed joints and PGRN's mild inhibition of neutrophils was independent of 14-3-3ε, indicating that the protection conferred by PGRN/TNFR2/14-3-3ε signaling in inflammatory arthritis was primarily attributable to their regulations of macrophage plasticity. Using macrophage-specific Cre system such as Cx3cr1-Cre (71) can further confirm the importance of macrophage-expressed 14-3-3ε in mediating PGRN/TNFR2 signaling, which warrants further investigations. Although loss of 14-3-3ε did not alter total macrophages in the inflamed joints of mice with CIA, studies with a lineage tracing system (CCR2 or Cx3cr1) and subsequent characterization of the macrophages in the joints can be performed to further confirm the findings that 14-3-3ε signaling does not affect the total number of macrophages in the joints of mice with CIA, although it plays an important role in regulating macrophage plasticity.

In addition to its crucial role in mediating macrophage polarization, TNFR2/14-3-3ε signaling also regulated T cell subtypes associated with inflammatory and autoimmune arthritis, such as Tregs and Th1 cells. PGRN exhibited a broader range of effects on T cells in terms of inducing anti-inflammatory Tregs and Th2 cells, while reducing pro-inflammatory Th17 and Th1 cells. Among these cell types, only the effects of PGRN on Tregs and Th1 depended on TNFR2/14-3-3ε, which might explain why PGRN's anti-inflammatory effects were almost abolished in global 14-3-3ε knockout mice. PGRN's influence on T cell populations was significantly compromised in myeloid-specific 14-3-3ε knockout mice, but did not reach the same degree of obstruction observed in the global 14-3-3ε knockout mice. This difference emphasized the importance of employing cell-specific deletion of 14-3-3ε to assess the role of 14-3-3ε in individual cell subsets in the pathogenesis of inflammatory and autoimmune arthritis.

Our comparative transcriptome profiling and GSEA analysis of WT and 14-3-3ε or PGRN knockout macrophages demonstrated that both 14-3-3ε and PGRN deletion rendered macrophage populations constitutively more inflamed than WT controls, supporting the scenario that 14-3-3ε-dependent TNFR2 signaling plays an immunoregulatory and anti-inflammatory role during inflammation. GSEA analysis also predicted that PI3K/Akt/mTOR and TNF signaling pathways may

be engaged in TNFR2/14-3-3ε regulation of macrophage polarization. Subsequent inhibition of the PI3k signaling pathway using its inhibitors and examination of the activation status of key signaling molecules involved in these pathways, along with DNA binding activity analysis, revealed that TNFR2/14-3-3ε signaled through PI3K/Akt/mTOR to restrict NF-κB activation and simultaneously stimulate C/EBPβ activation, thereby instructing macrophage functional plasticity to promote immune suppression (**Figure 9H**).

In summary, our study identified 14-3-3ε as an important regulator of macrophage plasticity which acted as a crucial co-factor of TNFR2 signaling. 14-3-3ε was necessary and sufficient to mediate TNFR2's regulation on macrophage polarization. TNFR2/14-3-3ε pathway represented a mechanism by which macrophage balanced between pro-inflammatory and anti-inflammatory responses and served as a promising candidate which could be targeted to regulate macrophage polarization. In addition, we also provided proof of principle for the potential of exogenous PGRN to promote anti-inflammation through regulating macrophage plasticity in the CIA model. These findings enable us to better understand the molecular mechanisms of TNFR2/14-3-3ε regulation of inflammatory and autoimmunity, and more excitingly, may provide a rational for targeting the beneficial TNFR2 signaling pathway as a novel therapeutic approach for inflammatory arthritis and other inflammatory and autoimmune diseases in which macrophage polarization plays key pathogenic roles.

Materials and Methods

Mice

TNFR2-/-, LysM-Cre, Rosa26a-CreERT2 mice were obtained from The Jackson Laboratory (Bar Harbor, ME, USA). 14-3-3$\varepsilon^{f/f}$ mice were provided by Dr. Kazuhito Toyo-oka, and mated with transgenic mice expressing LysM-Cre and Rosa26a-CreERT2 to obtain myeloid and global 14-3-3ε knockout mice, respectively. For activation of CreERT2 in adult mice, 150 mg/kg body weight of tamoxifen (Sigma-Aldrich, St. Louis, MO, USA) in sunflower seed oil (Sigma-Aldrich) was intraperitoneally injected into 10-week-old mice once a day for 5 consecutive days. Littermate controls were used for all experiments. Genotyping for these mice was performed by PCR as previously reported (45). PGRN-deficient mice were established and maintained by the laboratory (22). All animals were housed on a 12-hour light-dark cycle with ad libitum access to food and water in a specific pathogen–free environment. Animals were maintained on a B6 background and were sex- and age-matched for experiments, typically between 10- and 12-weeks-of-age.

Preparation of rhPGRN

Generation of our recombinant PGRN stable cell line and purification of recombinant PGRN have been described in our previous publication (72). In brief, stable cells were cultured in DMEM that contained 1 mg/ml G418. PGRN was affinity purified from the medium of starved cells by using nickel nitrilotriacetic-agarose. The purity of recombinant PGRN was determined by SDS-PAGE.

Collagen induced arthritis (CIA) model

Ten-week-old mice were immunized via 0.1-ml intradermal injection of 100 mg chicken type II collagen (Chondrex, Seattle, WA, USA) emulsified with an equal volume of Complete Freund's adjuvant (CFA) that contained 4 mg/ml heat denatured Mycobacterium (Chondrex) at the base of the tail (d0), followed by a booster immunization with chicken type II collagen emulsified in Incomplete

Freund's Adjuvant at day 19. In the CIA mouse model, clinical signs of arthritis in the paws were evaluated and scored individually by using a 0–4 point scoring system. Scores from each individual paw were summed to yield an overall score for each mouse, with a maximum score of 16 (73). Scores were attributed as follows: a paw score of 0, no signs; 1, mild swelling confined to the tarsal bones or ankle joint; 2, mild swelling extending from ankle to the tarsal bones; 3, moderate swelling extending from ankle to the metatarsal joints; and 4, severe swelling encompassing the ankle, foot, and digits and/or ankylosis of the limb. To determine therapeutic effects, recombinant PGRN (5 mg/kg body weight) was intraperitoneally injected into mice starting from day 20 after first immunization on alternating days until euthanasia. Incidence was taken as equal to the ratio of CIA mice to the total number of mice exposed to the emulsion injections, multiplied by 100.

Histological analysis of mouse joints

Mouse joint tissues were fixed in 4% paraformaldehyde, decalcified in EDTA, and embedded in paraffin. Tissue sections were then prepared and stained with hematoxylin and eosin (H&E). H&E-stained sections were scored for inflammation and bone erosion. Inflammation was scored according to the following criteria: 0, no inflammation; 1, slight thickening of the lining layer or some infiltrating cells in the underlying layer; 2, slight thickening of the lining layer plus some infiltrating cells in the underlying layer; 3, thickening of the lining layer, an influx of cells in the underlying layer, and presence of cells in the synovial space; and 4, synovium highly infiltrated with many inflammatory cells. Cartilage damage was determined by Safranin O staining, and the extent of cartilage damage was scored according to the following criteria: 0, no destruction; 1, minimal erosion limited to single spots; 2, slight-to-moderate erosion in a limited area; 3, more extensive erosion; and 4, general destruction (74). TRAP staining was used to determine bone erosion as previously described (22). The sections were imaged using a Zeiss microscope, and osteoclast quantification was performed using ImageJ software.

Immunohistochemistry staining

For immunohistochemistry staining, deparaffinized and hydrated sections were incubated with 0.1% trypsin for 30min at 37°C, followed by 0.25 U/ml chondroitinase ABC (Sigma-Aldrich) and 1 U/ml hyaluronidase (Sigma-Aldrich) for 60min at 37°C, respectively. Then the sections were incubated with antibodies against myeloperoxidase (1:100, PA5-16672, Invitrogen) overnight at 4°C. Detection was performed using the Vectastain Elite ABC kit (Vector, CA and positive signal was visualized with 0.5 mg/ml 3,3-diaminobenzidine in 50 mM Tris-Cl substrate (Sigma-Aldrich) and counterstained with 1% methyl green. Images were acquired with a Zeiss microscope.

Flow cytometry analysis

Single-cell suspensions from joint, spleen or BMDMs were subjected to flow cytometry analysis. To prepare the single cell suspensions from joints, the hind paws were harvested as previously described. (75, 76). After the skins were removed, the paws were minced and digested in digestion buffer (2mg/ml collagenase D, 2mg/ml diapause II, and 1mg/ml DNase I in HBSS) for 60min at 37°C. Antibodies used were FITC conjugated anti-CD4 (GK1.5), APC conjugated anti-CD25 (PC61.5), eFluor 450 conjugated anti-IL-17 (eBio17B7), PE conjugated anti-IL-4 (11B11), APC-CY™7 conjugated IFNγ (XMG1.2), biotin conjugated anti-Foxp3 (FJK-16s), FITC conjugated CD11b (M1/70), eFluor450 conjugated anti-CD45 (30-F11), APC conjugated iNOS (CXNFT), PE conjugated anti-CD206 (MMR), PE-cyanine5 conjugated anti-CD4 (RM4-5) from eBioscience (San Diego, CA,USA); and streptavidin-conjugated Qdot 605 from Thermo Fisher Scientific (Waltham, MA, USA). For myeloid progenitor experiments, bone marrow cells were stained with the following antibodies for lineage markers (CE3e (145-2C11) PE-cyanine7, B220 (RA3-6B2) PE-cyanine7, CD14 (Sa14-2) PE-cyanine7, CD4 (GK1.5) PE-cyanine7, CD8 (53-6.7) PE-cyanine7, Ter119 (TER-119) PE-cyanine7, Gr1 (RB6-8C5) PE-cyanine7), CD16/32 (93) APC, cKit (2B8) APC-eFluor780, Scal (D7) Pacific Blue, CD34 (RAM34) FITC and IL-

7Rα (A7R34) PE-cyanine5. Cells were acquired using BD LSR Fortessa and analyzed by FlowJo and FCS Express.

Determining the proliferative capacity of cells

To assess cell proliferation in the joints of mice with CIA, EdU was injected into the mice at 50mg/kg body weight twice per week for a week before sacrifice the mice as previously described (77). After isolating cells from the joints, Click-iT EdU kit from Invitrogen with Alexa Fluor 488 was used to detect the incorporated EdU as per manufacturer's guidelines.

Determining LysM-Cre deletion efficiency in macrophages of the inflamed joints

Macrophages were purified from arthritic joins of 14-3-3$\varepsilon^{f/f}$ and 14-3-3ε^{LysM} CIA mice using MagniSort mouse F4/80 positive selection kit (Invitrogen). DNA extracted from the purified macrophages was used as template to detect the 14-3-3ε floxed allele and knockout band as previously reported (45).

Generation of 14-3-3ε KO and PGRN KO Raw264.7 by CRISPR-Cas9

Knockout cells were generated in accordance with a previously published protocol (78). Briefly, 14-3-3ε or PGRN sgRNA was inserted into the lentiCRISPR V2 vector (Addgene, Watertown, MA, USA). Co-transfection of CRISPR plasmid, psPAX2 and pMD2.G (Addgene) into HEK293T (ATCC) to produce the lentivirus. Then Raw264.7 (ATCC, Gaithersburg, MD, USA) were infected with the collected lentivirus for 18h, followed by selection with 2μg/ml puromycin (Gibco, Gaithersburg, MD, USA) for 2 days.

Isolation of bone marrow derived macrophages (BMDMs) and neutrophils and differentiation of BMDMs

Bone marrow cells were collected from the mice and cultured in α-MEM supplemented with 10% FBS

and 10ng/ml M-CSF (Biolegend, San Diego, CA, USA) over 7 days for macrophage differentiation. Differentiated BMDMs were stimulated with 100ng/ml LPS (Sigma-Aldrich) + 20ng/ml IFNy (Peprotech) or 20ng/ml IL-4 (Peprotech, Rocky Hill, NJ, USA) for 18h to polarize cells to M1 or M2 macrophage in the presence or absence of PGRN or TY010 (kindly provided by Dr. Denise Faustman at Harvard Medical School, Boston, MA), respectively. For inhibitor studies, PI3K inhibitor wortmannin (100nM, Sigma-Aldrich) or mTOR inhibitor rapamycin (100nM, Sigma-Aldrich) were incubated with macrophages for 1h before the addition of polarizing stimuli.

Bone marrow neutrophils were isolated by the negative selection technique using an EasySep Mouse Neutrophil Enrichment Kit (Stemcell Technologies).

Osteoclast differentiation and TRAP staining

BMDMs were obtained as described above and cultured with α-MEM supplemented with 10% fetal bovine serum, 10ng/ml M-CSF, 50ng/ml RNAKL (R&D), 20ng/ml TNFα and 500ng/ml PGRN for 5 days. The medium was replaced every day. TRAP staining was performed and the number of TRAP positive multi-nucleated cells (TRAP+-MNCs) containing more than three nuclei were counted using microscopy as described (*22*).

RNA-seq and bioinformatics analysis

Freshly isolated mouse bone marrow cells from nine WT, nine 14-3-3ε^{LysM} and nine PGRN−/− mice were pooled into three replicate sets of WT, 14-3-3ε^{LysM} and PGRN−/− cells and differentiated into macrophages for 7 days in α-MEM supplemented with 10%FBS and 10ng/ml M-CSF. Each replicate set of macrophages was then treated with IL4 or IFNγ /LPS. Total RNA was extracted from BMDMs with RNeasy Mini Kit (Qiagen, Germantown, MD, USA). mRNA was isolated from purified DNA-free RNA for library preparation. Libraries were sequenced on Illumina HiSeq 4000 by the NYU Genome Technology Center. Reads for genes were called using RSEM program (79) and differentially

expressed genes were discovered using DESeq2 package (80). Significantly differentially expressed genes were defined by a 2-fold change with a false discovery ratio (FDR) ≤ 0.05. Genes which were significantly up- and down-regulated in 14-3-3ε^{Lysm} compared to 14-3-3ε$^{f/f}$ and were implicated in TNFα and PI3K/Akt/mTOR pathways were used for transcription factor enrichment analysis with TFactS (57). All RNA-seq datasets used in this study have been deposited in the NCBI's Gene Expression Omnibus database (GEO GSE172119).

Individual quantitative RT–PCR

Total RNA was extracted from BMDMs with the RNeasy Mini Kit (Qiagen). cDNA was prepared using 1 μg RNA with the High-Capacity cDNA Reverse Transcription Kit (Applied Biosystems, Foster City, CA, USA). SYBR green (Applied Biosystems) based qPCR was performed in triplicate using human and mouse primers to *Arg1*, *Mgl1*, *Il6*, *Nos2*, and *Gapdh* (Applied Biosystems Real-time PCR system). mRNA levels were normalized to *Gapdh* and reported as relative mRNA fold change.

Transcription factor DNA Binding assays

NF-kB p65 and C/EBPβ DNA binding activity were measured by TransAM transcription factor assay kits (43296 and 44196, Active Motif, Carlsbad, CA, USA). WT, 14-3-3ε^{LysM} and PGRN−/− BMDMs were stimulated with 100 ng/ml LPS + 20 ng/ml IFNγ or 20 ng/ml for the indicated time, and nuclear extracts were prepared in lysis buffer AM2 (Active Motif). Nuclear extracts were incubated with the immobilized consensus sequence and p65 or C/EBPβ was detected using specific antibodies. For competitive binding studies, functional (oligo) or nonfunctional (mutant oligo) oligonucleotides were used according to the manufacturer's instructions.

Biochemical co-purification and mass spectrometry

To isolate the co-factors of the PGRN/TNFR2 complex that mediate the intracellular signaling through

TNFR2, the intracellular domain (ICD) of TNFR2 was cloned into the PGEX-3X vector to express a fusion of GST to TNFR2ICD. GST (serving as a control) or GST-TNFR2ICD was affinity-purified on glutathione-agarose beads and used as a bait to trap proteins from RAW264.7 cells treated with 500ng/ml PGRN for 30min. These samples were then analyzed by mass spectrometry, performed by NYU Proteomics Laboratory. All MS/MS spectra were collected using the following instrument parameters: resolution of 15,000, AGC target of 1e5, maximum ion time of 120 ms, one microscan, 2 m/z isolation window, fixed first mass of 150 m/z, and NCE of 27. MS/MS spectra were searched against a Uniprot Human database using Sequest within Proteome Discoverer 1.4.

Immunoprecipitation

BMDMs isolated from 14-3-3$\varepsilon^{f/f}$ and 14-3-3ε^{LysM} mice or control and 14-3-3ε KO Raw264.7 macrophages were treated with PGRN for 30min prior to lysis in RIPA buffer containing protease inhibitors. 400μg of total protein were immunoprecipitated with anti-14-3-3ε antibody, the protein complexes were detected with anti-TNFR2 and 14-3-3ε antibodies.

Immunoblotting

IL-4 and LPS treated macrophage cultures were solubilized in RIPA buffer containing protease and phosphatase inhibitors. 50 μg of total protein was separated by SDS-PAGE and electroblotted onto NC membranes (Bio-Rad Laboratories, Hercules, CA, USA) using a wet transfer system. Proteins were detected by incubation with 1:1,000 dilutions of primary antibodies, washed and incubated with appropriate secondary antibodies and detected after incubation with a chemiluminescent substrate. Primary antibodies against Akt (9272), p-AKT Thr308 (4056), p-Akt Ser473 (4058), IκKα (2682), IκKβ (8943), p-IκKα/β (2697), p65 (4764), p-p65 (3033), C/EBPβ (3087), p-CEBPβ (3084) were purchased from Cell Signaling Technology, and 14-3-3ε (sc-393177), PGRN (sc-28928) and TNFR2 (sc-7862) antibodies were purchased from Santa Cruz Biotechnology.

ELISA assay

Levels of IL-6, IL-1β, TNFα, IL-17 and IL-10 were detected in sera isolated from murine models using ELISA kits in accordance with manufacturer's instructions (Invitrogen).

Statistical analyses

The numbers of mice used per genotype are indicated in figure legends. Comparisons between two groups were analyzed using 2-tailed unpaired Student's t-tests. One-way ANOVA with post hoc Bonferroni test was used when comparing multiple groups. A value of $P < 0.05$ was considered statistically significant.

Study approval

All animal studies were performed in accordance with institutional guidelines and approved by the Institutional Animal Care and Use Committee of New York University School of Medicine.

Author contributions

W.F. and C-J.L. designed the experiments and wrote the manuscript. W.F. executed most experiments. W.H. performed RNA-seq analysis and assisted with flow cytometry analysis. Y.Y. assisted with protein immunoprecipitation. A.H., G.S., Y.B., W.H., L.Z., G.G., and J.L. assisted with protein purification and animal experiments. K.T. provided 14-3-3$\varepsilon^{f/f}$ mice. D.S., G.X. and P.L. participated in analyzing the data and editing the manuscript.

Acknowledgement

This work was supported partly by NIH research grants R01AR062207, R01AR061484, R01AR076900, R01NS103931, R01NS096098 and a DOD research grant W81XWH-16-1-0482. Authors would like to acknowledge all lab members for the insightful discussions. We greatly appreciate Dr. Denise Faustman at Harvard Medical School for providing TNFR2 agonist TY010. We also thank the NYU Genome Technology Center and Proteomics Laboratory for technical support.

Reference

1. Scott DL, Wolfe F, and Huizinga TW. Rheumatoid arthritis. *Lancet.* 2010;376(9746):1094-108.
2. Kinne RW, Stuhlmuller B, and Burmester GR. Cells of the synovium in rheumatoid arthritis. Macrophages. *Arthritis Res Ther.* 2007;9(6):224.
3. Udalova IA, Mantovani A, and Feldmann M. Macrophage heterogeneity in the context of rheumatoid arthritis. *Nat Rev Rheumatol.* 2016;12(8):472-85.
4. Siouti E, and Andreakos E. The many facets of macrophages in rheumatoid arthritis. *Biochem Pharmacol.* 2019;165:152-69.
5. Funes SC, Rios M, Escobar-Vera J, and Kalergis AM. Implications of macrophage polarization in autoimmunity. *Immunology.* 2018;154(2):186-95.
6. Tabas I, and Glass CK. Anti-inflammatory therapy in chronic disease: challenges and opportunities. *Science.* 2013;339(6116):166-72.
7. Wynn TA, Chawla A, and Pollard JW. Macrophage biology in development, homeostasis and disease. *Nature.* 2013;496(7446):445-55.
8. Wang N, Liang H, and Zen K. Molecular mechanisms that influence the macrophage m1-m2 polarization balance. *Frontiers in immunology.* 2014;5:614.
9. Mantovani A, Sica A, Sozzani S, Allavena P, Vecchi A, and Locati M. The chemokine system in diverse forms of macrophage activation and polarization. *Trends Immunol.* 2004;25(12):677-86.
10. Sedger LM, and McDermott MF. TNF and TNF-receptors: From mediators of cell death and inflammation to therapeutic giants - past, present and future. *Cytokine Growth Factor Rev.* 2014;25(4):453-72.
11. Williams A, Wang EC, Thurner L, and Liu CJ. Review: Novel Insights Into Tumor Necrosis Factor Receptor, Death Receptor 3, and Progranulin Pathways in Arthritis and Bone Remodeling. *Arthritis & rheumatology.* 2016;68(12):2845-56.
12. Keffer J, Probert L, Cazlaris H, Georgopoulos S, Kaslaris E, Kioussis D, et al. Transgenic mice expressing human tumour necrosis factor: a predictive genetic model of arthritis. *Embo J.* 1991;10(13):4025-31.
13. Bluml S, Scheinecker C, Smolen JS, and Redlich K. Targeting TNF receptors in rheumatoid arthritis. *International immunology.* 2012;24(5):275-81.
14. Peschon JJ, Torrance DS, Stocking KL, Glaccum MB, Otten C, Willis CR, et al. TNF receptor-deficient mice reveal divergent roles for p55 and p75 in several models of inflammation. *J Immunol.* 1998;160(2):943-52.
15. Cui Y, Hettinghouse A, and Liu CJ. Progranulin: A conductor of receptors orchestra, a chaperone of lysosomal enzymes and a therapeutic target for multiple diseases. *Cytokine Growth Factor Rev.* 2019;45:53-64.
16. Tseng WY, Huang YS, Clanchy F, McNamee K, Perocheau D, Ogbechi J, et al. TNF receptor 2 signaling prevents DNA methylation at the Foxp3 promoter and prevents pathogenic conversion of regulatory T cells. *Proc Natl Acad Sci U S A.* 2019;116(43):21666-72.
17. Monaco C, Nanchahal J, Taylor P, and Feldmann M. Anti-TNF therapy: past, present and future. *Int Immunol.* 2015;27(1):55-62.
18. Muller J, Baeyens A, and Dustin ML. Tumor Necrosis Factor Receptor Superfamily in T Cell Priming and Effector Function. *Adv Immunol.* 2018;140:21-57.
19. Bluml S, Binder NB, Niederreiter B, Polzer K, Hayer S, Tauber S, et al. Antiinflammatory effects of tumor necrosis factor on hematopoietic cells in a murine model of erosive arthritis. *Arthritis Rheum.* 2010;62(6):1608-19.
20. Ruspi G, Schmidt EM, McCann F, Feldmann M, Williams RO, Stoop AA, et al. TNFR2 increases the sensitivity of ligand-induced activation of the p38 MAPK and NF-kappaB pathways and signals TRAF2 protein degradation in macrophages. *Cellular signalling.*

2014;26(4):683-90.
21. Sheng Y, Li F, and Qin Z. TNF Receptor 2 Makes Tumor Necrosis Factor a Friend of Tumors. *Front Immunol.* 2018;9:1170.
22. Tang W, Lu Y, Tian QY, Zhang Y, Guo FJ, Liu GY, et al. The Growth Factor Progranulin Binds to TNF Receptors and Is Therapeutic Against Inflammatory Arthritis in Mice. *Science.* 2011;332(6028):478-84.
23. Liu CJ. Progranulin: a promising therapeutic target for rheumatoid arthritis. *FEBS Lett.* 2011;585(23):3675-80.
24. Liu CJ, and Bosch X. Progranulin: A growth factor, a novel TNFR ligand and a drug target. *Pharmacology & therapeutics.* 2012;133(1):124-32.
25. Wei F, Zhang Y, Jian J, Mundra JJ, Tian Q, Lin J, et al. PGRN protects against colitis progression in mice in an IL-10 and TNFR2 dependent manner. *Scientific reports.* 2014;4:7023.
26. Fu W, Hu W, Shi L, Mundra JJ, Xiao G, Dustin ML, et al. Foxo4- and Stat3-dependent IL-10 production by progranulin in regulatory T cells restrains inflammatory arthritis. *FASEB J.* 2017;31(4):1354-67.
27. Zhao YP, Liu B, Tian QY, Wei JL, Richbourgh B, and Liu CJ. Progranulin protects against osteoarthritis through interacting with TNF-alpha and beta-Catenin signalling. *Ann Rheum Dis.* 2015;74(12):2244-53.
28. Zhang K, Li YJ, Guo Y, Zheng KY, Yang Q, Yang L, et al. Elevated progranulin contributes to synaptic and learning deficit due to loss of fragile X mental retardation protein. *Brain.* 2017;140(12):3215-32.
29. Huang K, Chen A, Zhang X, Song Z, Xu H, Cao J, et al. Progranulin is preferentially expressed in patients with psoriasis vulgaris and protects mice from psoriasis-like skin inflammation. *Immunology.* 2015;145(2):279-87.
30. Vezina A, Vaillancourt-Jean E, Albarao S, and Annabi B. Mesenchymal stromal cell ciliogenesis is abrogated in response to tumor necrosis factor-alpha and requires NF-kappaB signaling. *Cancer letters.* 2014;345(1):100-5.
31. Zhou M, Tang W, Fu Y, Xu X, Wang Z, Lu Y, et al. Progranulin protects against renal ischemia/reperfusion injury in mice. *Kidney international.* 2015;87(5):918-29.
32. Li H, Zhou B, Xu L, Liu J, Zang W, Wu S, et al. Circulating PGRN is significantly associated with systemic insulin sensitivity and autophagic activity in metabolic syndrome. *Endocrinology.* 2014;155(9):3493-507.
33. Yang D, Wang LL, Dong TT, Shen YH, Guo XS, Liu CY, et al. Progranulin promotes colorectal cancer proliferation and angiogenesis through TNFR2/Akt and ERK signaling pathways. *American journal of cancer research.* 2015;5(10):3085-97.
34. Liu J, Li H, Zhou B, Xu L, Kang X, Yang W, et al. PGRN induces impaired insulin sensitivity and defective autophagy in hepatic insulin resistance. *Molecular endocrinology.* 2015;29(4):528-41.
35. Kadl A, Meher AK, Sharma PR, Lee MY, Doran AC, Johnstone SR, et al. Identification of a novel macrophage phenotype that develops in response to atherogenic phospholipids via Nrf2. *Circ Res.* 2010;107(6):737-46.
36. Adamson SE, Griffiths R, Moravec R, Senthivinayagam S, Montgomery G, Chen W, et al. Disabled homolog 2 controls macrophage phenotypic polarization and adipose tissue inflammation. *J Clin Invest.* 2016;126(4):1311-22.
37. Wei F, Zhang Y, Zhao W, Yu X, and Liu CJ. Progranulin Facilitates Conversion and Function of Regulatory T Cells under Inflammatory Conditions. *PloS one.* 2014;9(11):e112110.
38. Okubo Y, Mera T, Wang L, and Faustman DL. Homogeneous expansion of human T-regulatory cells via tumor necrosis factor receptor 2. *Sci Rep.* 2013;3:3153.
39. Aitken A, Jones D, Soneji Y, and Howell S. 14-3-3 proteins: biological function and domain

structure. *Biochem Soc Trans.* 1995;23(3):605-11.
40. Fu H, Subramanian RR, and Masters SC. 14-3-3 proteins: structure, function, and regulation. *Annu Rev Pharmacol Toxicol.* 2000;40:617-47.
41. Barry EF, Felquer FA, Powell JA, Biggs L, Stomski FC, Urbani A, et al. 14-3-3:Shc scaffolds integrate phosphoserine and phosphotyrosine signaling to regulate phosphatidylinositol 3-kinase activation and cell survival. *J Biol Chem.* 2009;284(18):12080-90.
42. Dougherty MK, and Morrison DK. Unlocking the code of 14-3-3. *J Cell Sci.* 2004;117(Pt 10):1875-84.
43. Aitken A. 14-3-3 proteins: a historic overview. *Semin Cancer Biol.* 2006;16(3):162-72.
44. Mackintosh C. Dynamic interactions between 14-3-3 proteins and phosphoproteins regulate diverse cellular processes. *Biochem J.* 2004;381(Pt 2):329-42.
45. Toyo-oka K, Wachi T, Hunt RF, Baraban SC, Taya S, Ramshaw H, et al. 14-3-3epsilon and zeta regulate neurogenesis and differentiation of neuronal progenitor cells in the developing brain. *J Neurosci.* 2014;34(36):12168-81.
46. Clausen BE, Burkhardt C, Reith W, Renkawitz R, and Forster I. Conditional gene targeting in macrophages and granulocytes using LysMcre mice. *Transgenic Res.* 1999;8(4):265-77.
47. Ventura A, Kirsch DG, McLaughlin ME, Tuveson DA, Grimm J, Lintault L, et al. Restoration of p53 function leads to tumour regression in vivo. *Nature.* 2007;445(7128):661-5.
48. Wei S, Kitaura H, Zhou P, Ross FP, and Teitelbaum SL. IL-1 mediates TNF-induced osteoclastogenesis. *J Clin Invest.* 2005;115(2):282-90.
49. Wu L, Guo Q, Yang J, and Ni B. Tumor Necrosis Factor Alpha Promotes Osteoclast Formation Via PI3K/Akt Pathway-Mediated Blimp1 Expression Upregulation. *J Cell Biochem.* 2017;118(6):1308-15.
50. Chitramuthu BP, Bennett HPJ, and Bateman A. Progranulin: a new avenue towards the understanding and treatment of neurodegenerative disease. *Brain.* 2017;140(12):3081-104.
51. Covarrubias AJ, Aksoylar HI, and Horng T. Control of macrophage metabolism and activation by mTOR and Akt signaling. *Semin Immunol.* 2015;27(4):286-96.
52. Fukao T, and Koyasu S. PI3K and negative regulation of TLR signaling. *Trends Immunol.* 2003;24(7):358-63.
53. Troutman TD, Bazan JF, and Pasare C. Toll-like receptors, signaling adapters and regulation of the pro-inflammatory response by PI3K. *Cell Cycle.* 2012;11(19):3559-67.
54. Kaneda MM, Messer KS, Ralainirina N, Li H, Leem CJ, Gorjestani S, et al. PI3Kgamma is a molecular switch that controls immune suppression. *Nature.* 2016;539(7629):437-42.
55. Katholnig K, Linke M, Pham H, Hengstschlager M, and Weichhart T. Immune responses of macrophages and dendritic cells regulated by mTOR signalling. *Biochem Soc Trans.* 2013;41(4):927-33.
56. Wang S, Liu R, Yu Q, Dong L, Bi Y, and Liu G. Metabolic reprogramming of macrophages during infections and cancer. *Cancer Lett.* 2019;452:14-22.
57. Essaghir A, Toffalini F, Knoops L, Kallin A, van Helden J, and Demoulin JB. Transcription factor regulation can be accurately predicted from the presence of target gene signatures in microarray gene expression data. *Nucleic Acids Res.* 2010;38(11):e120.
58. Weichhart T, and Saemann MD. The multiple facets of mTOR in immunity. *Trends Immunol.* 2009;30(5):218-26.
59. Luyendyk JP, Schabbauer GA, Tencati M, Holscher T, Pawlinski R, and Mackman N. Genetic analysis of the role of the PI3K-Akt pathway in lipopolysaccharide-induced cytokine and tissue factor gene expression in monocytes/macrophages. *J Immunol.* 2008;180(6):4218-26.
60. Sahin E, Haubenwallner S, Kuttke M, Kollmann I, Halfmann A, Dohnal AM, et al. Macrophage PTEN regulates expression and secretion of arginase I modulating innate and adaptive immune responses. *J Immunol.* 2014;193(4):1717-27.

61. Ben-Neriah Y, and Karin M. Inflammation meets cancer, with NF-kappaB as the matchmaker. *Nat Immunol.* 2011;12(8):715-23.
62. Bonizzi G, and Karin M. The two NF-kappaB activation pathways and their role in innate and adaptive immunity. *Trends Immunol.* 2004;25(6):280-8.
63. Gray MJ, Poljakovic M, Kepka-Lenhart D, and Morris SM, Jr. Induction of arginase I transcription by IL-4 requires a composite DNA response element for STAT6 and C/EBPbeta. *Gene.* 2005;353(1):98-106.
64. El Kasmi KC, Qualls JE, Pesce JT, Smith AM, Thompson RW, Henao-Tamayo M, et al. Toll-like receptor-induced arginase 1 in macrophages thwarts effective immunity against intracellular pathogens. *Nat Immunol.* 2008;9(12):1399-406.
65. Tardito S, Martinelli G, Soldano S, Paolino S, Pacini G, Patane M, et al. Macrophage M1/M2 polarization and rheumatoid arthritis: A systematic review. *Autoimmun Rev.* 2019;18(11):102397.
66. Priam S, Bougault C, Houard X, Gosset M, Salvat C, Berenbaum F, et al. Identification of soluble 14-3-3 as a novel subchondral bone mediator involved in cartilage degradation in osteoarthritis. *Arthritis Rheum.* 2013;65(7):1831-42.
67. Yan W, Ding A, Kim HJ, Zheng H, Wei F, and Ma X. Progranulin Controls Sepsis via C/EBPalpha-Regulated Il10 Transcription and Ubiquitin Ligase/Proteasome-Mediated Protein Degradation. *J Immunol.* 2016;197(8):3393-405.
68. Williams RO, Feldmann M, and Maini RN. Anti-tumor necrosis factor ameliorates joint disease in murine collagen-induced arthritis. *Proc Natl Acad Sci U S A.* 1992;89(20):9784-8.
69. Ohshima S, Saeki Y, Mima T, Sasai M, Nishioka K, Nomura S, et al. Interleukin 6 plays a key role in the development of antigen-induced arthritis. *Proc Natl Acad Sci U S A.* 1998;95(14):8222-6.
70. Boe A, Baiocchi M, Carbonatto M, Papoian R, and Serlupi-Crescenzi O. Interleukin 6 knock-out mice are resistant to antigen-induced experimental arthritis. *Cytokine.* 1999;11(12):1057-64.
71. Yona S, Kim KW, Wolf Y, Mildner A, Varol D, Breker M, et al. Fate mapping reveals origins and dynamics of monocytes and tissue macrophages under homeostasis. *Immunity.* 2013;38(1):79-91.
72. Feng JQ, Guo FJ, Jiang BC, Zhang Y, Frenkel S, Wang DW, et al. Granulin epithelin precursor: a bone morphogenic protein 2-inducible growth factor that activates Erk1/2 signaling and JunB transcription factor in chondrogenesis. *FASEB J.* 2010;24(6):1879-92.
73. Brand DD, Latham KA, and Rosloniec EF. Collagen-induced arthritis. *Nat Protoc.* 2007;2(5):1269-75.
74. Camps M, Ruckle T, Ji H, Ardissone V, Rintelen F, Shaw J, et al. Blockade of PI3Kgamma suppresses joint inflammation and damage in mouse models of rheumatoid arthritis. *Nat Med.* 2005;11(9):936-43.
75. Li J, Zhang L, Zheng Y, Shao R, Liang Q, Yu W, et al. BAD inactivation exacerbates rheumatoid arthritis pathology by promoting survival of sublining macrophages. *Elife.* 2020;9.
76. Misharin AV, Cuda CM, Saber R, Turner JD, Gierut AK, Haines GK, 3rd, et al. Nonclassical Ly6C(-) monocytes drive the development of inflammatory arthritis in mice. *Cell Rep.* 2014;9(2):591-604.
77. Murphy MP, Koepke LS, Lopez MT, Tong X, Ambrosi TH, Gulati GS, et al. Articular cartilage regeneration by activated skeletal stem cells. *Nat Med.* 2020;26(10):1583-92.
78. Ran FA, Hsu PD, Wright J, Agarwala V, Scott DA, and Zhang F. Genome engineering using the CRISPR-Cas9 system. *Nat Protoc.* 2013;8(11):2281-308.
79. Li B, and Dewey CN. RSEM: accurate transcript quantification from RNA-Seq data with or without a reference genome. *BMC Bioinformatics.* 2011;12:323.
80. Love MI, Huber W, and Anders S. Moderated estimation of fold change and dispersion for

RNA-seq data with DESeq2. *Genome Biol.* 2014;15(12):550.

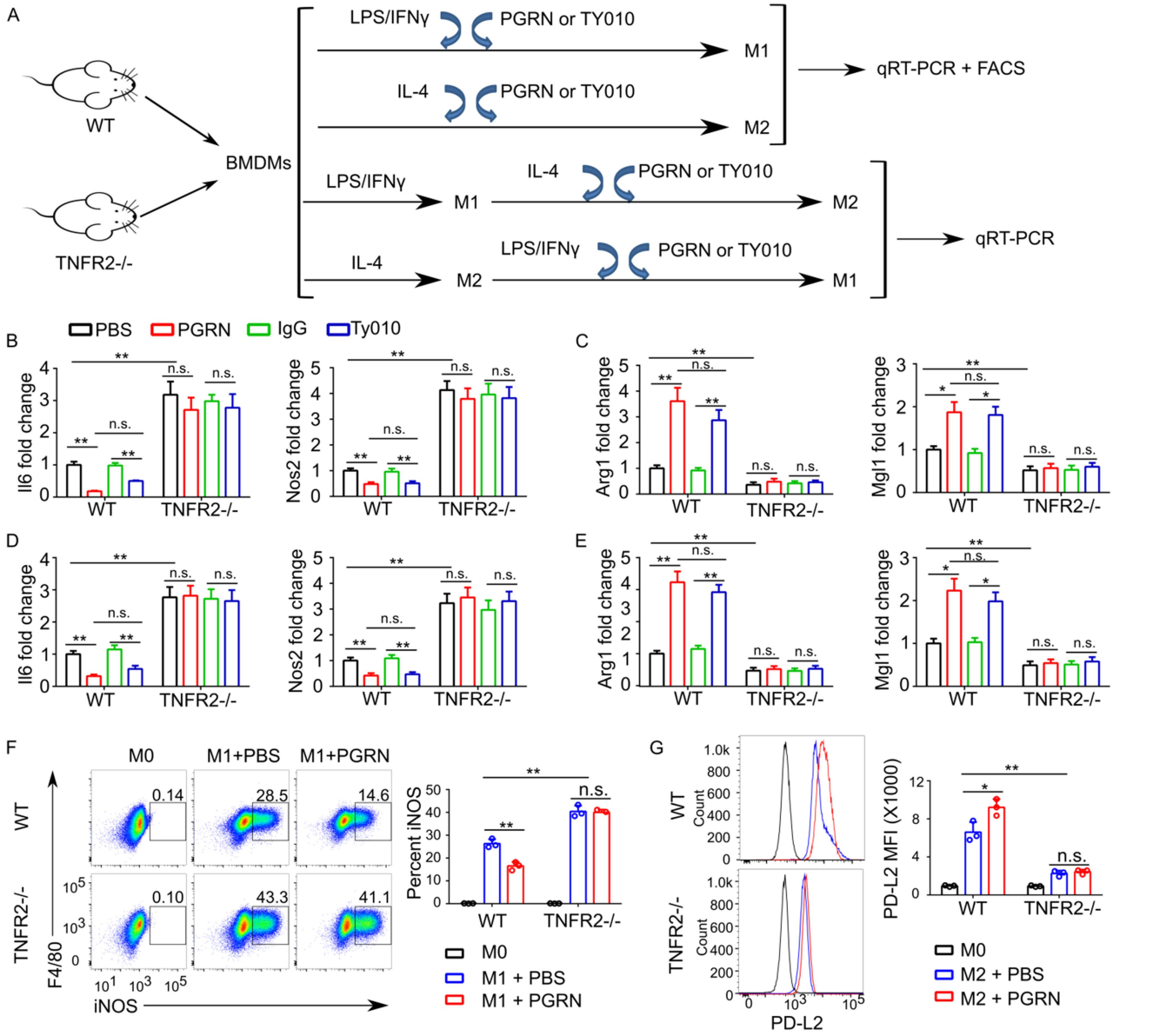

Fig.1 TNFR2 signaling controls macrophage polarization. (A) Schematic diagram illustrating the in vitro experimental design. (**B**) Fold change of *Il6* and *Nos2* mRNA in WT and TNFR2-/- BMDMs polarized to M1 with LPS/IFNγ in the presence or absence of 0.5μg/ml PGRN or 2.5 μg/ml TY010 for 18h. (**C**) Fold change of *Arg1* and *Mgl1* mRNA in WT and TNFR2-/- BMDMs polarized to M2 with IL-4 in the presence or absence of 0.5μg/ml PGRN or 2.5 μg/ml TY010 for 18h. (**D, E**) BMDMs from WT and TNFR2-/- were polarized to M2 (IL-4) or M1 (LPS/IFNγ) for 18 hours. Media were removed and M2 macrophages were treated with M1 stimuli (LPS/IFNγ) while M1 macrophages were treated with M2 stimuli (IL-4) with or without of 0.5μg/ml PGRN or 2.5 μg/ml TY010for an additional 18h. qPCR was performed to measure the expression of *Nos2* and *Il6*in M2 macrophages polarized to M1 (D), and the expression of *Arg1* and *Mgl1*in M1 macrophages polarized to M2 (E). (**F, G**) Flow cytometry analysis of WT and TNFR2-/- BMDMs polarized to M1 (F) or M2 (G) in the absence and presence of PGRN. CD45+CD11b+ cells were gated, and iNOS+ cells or PD-L2 mean fluorescence intensity (MFI) were analyzed. Data are mean ± SD; n = 3 biological replicates; significant difference was analyzed by one-way ANOVA with post hoc Bonferroni test; **P* < 0.05 or ***P* < 0.01.

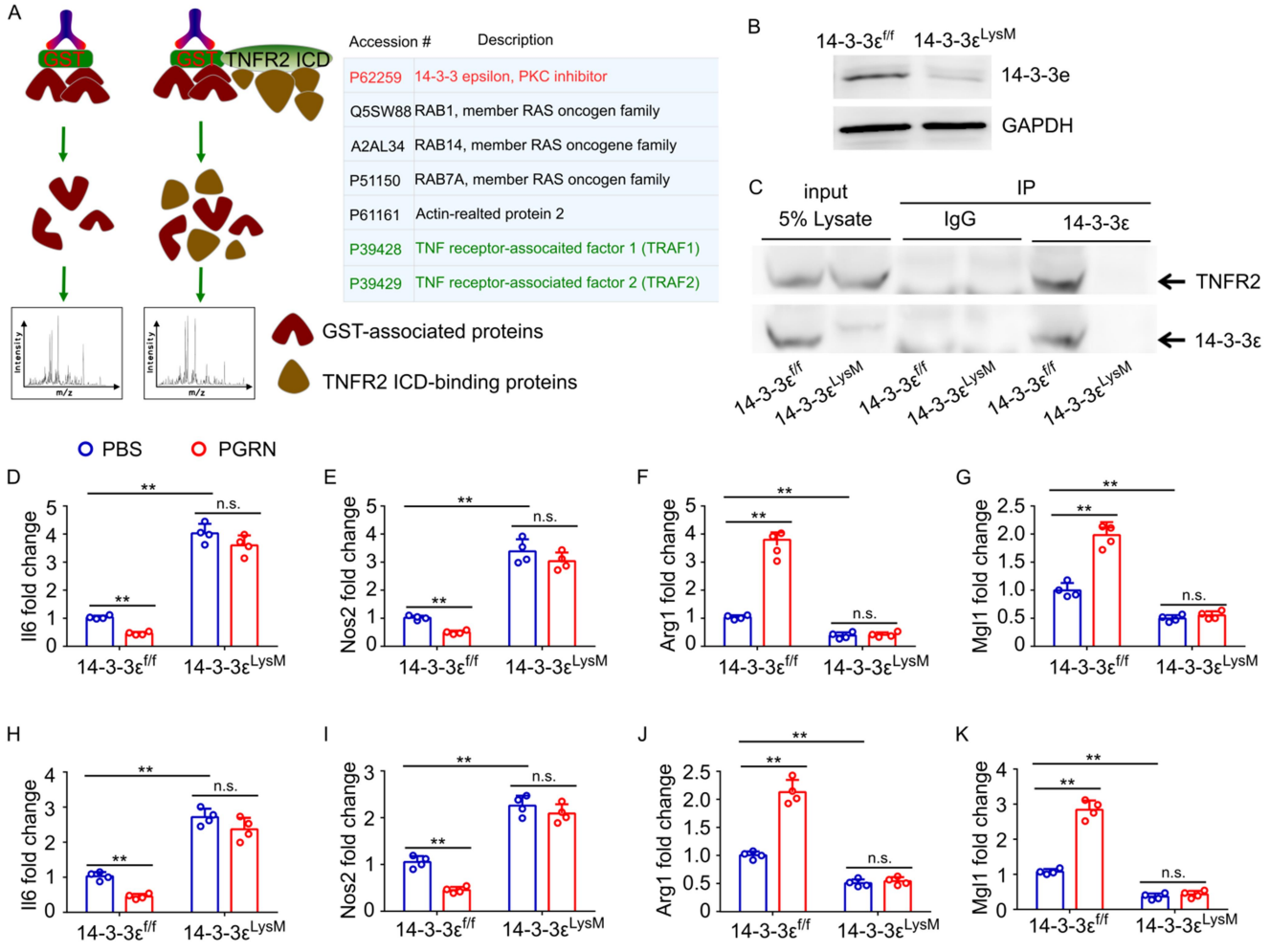

Fig. 2 Activation of TNFR2 recruits 14-3-3ε during macrophage polarization. (**A**) Experimental design to identify potential molecules binding to TNFR2ICD upon PGRN stimulation. Summary of the hits that were specifically recruited to activated TNFR2 complexes in Raw264.7 macrophages. (**B**) Efficient ablation of 14-3-3ε in 14-3-3ε^{LysM} BMDMs, assayed by Western blotting. (**C**) Immunoprecipitation from 14-3-3ε$^{f/f}$ or 14-3-3ε^{LysM} BMDMs with 14-3-3ε antibody and detection of TNFR2 and 14-3-3ε by immunoblotting. Results shown are representative of 3 biological replicates. (**D-G**) 14-3-3ε$^{f/f}$ and 14-3-3ε^{LysM} BMDMs were polarized to M1 (LPS/IFNγ) or M2 (IL-4) with or without 0.5μg/ml PGRN for 18h, qPCR was performed to measure the expression of *Il6* (**D**), *Nos2* (**E**), *Arg1*(**F**) and *Mgl1* (**G**). (H-K) 14-3-3ε$^{f/f}$ and 14-3-3ε^{LysM} BMDMs were polarized to M2 (IL-4) or M1 (LPS/IFNγ) for 18 hours, then M2 macrophages were treated with M1 stimuli (LPS/IFNγ) while M1 macrophages were treated with M2 stimuli (IL-4) for an additional 18h. qPCR was performed to measure the expression of *Il6* (**H**) and *Nos2*(**I**) in M2 macrophages polarized to M1; Expression of *Arg1*(**J**) and *Mgl1* (**K**) were measured in M1 macrophages polarized to M2. D-K, data are mean ± SD; n = 4 biological replicates; significant difference was analyzed by one-way ANOVA with post hoc Bonferroni test; $^{**}P < 0.01$.

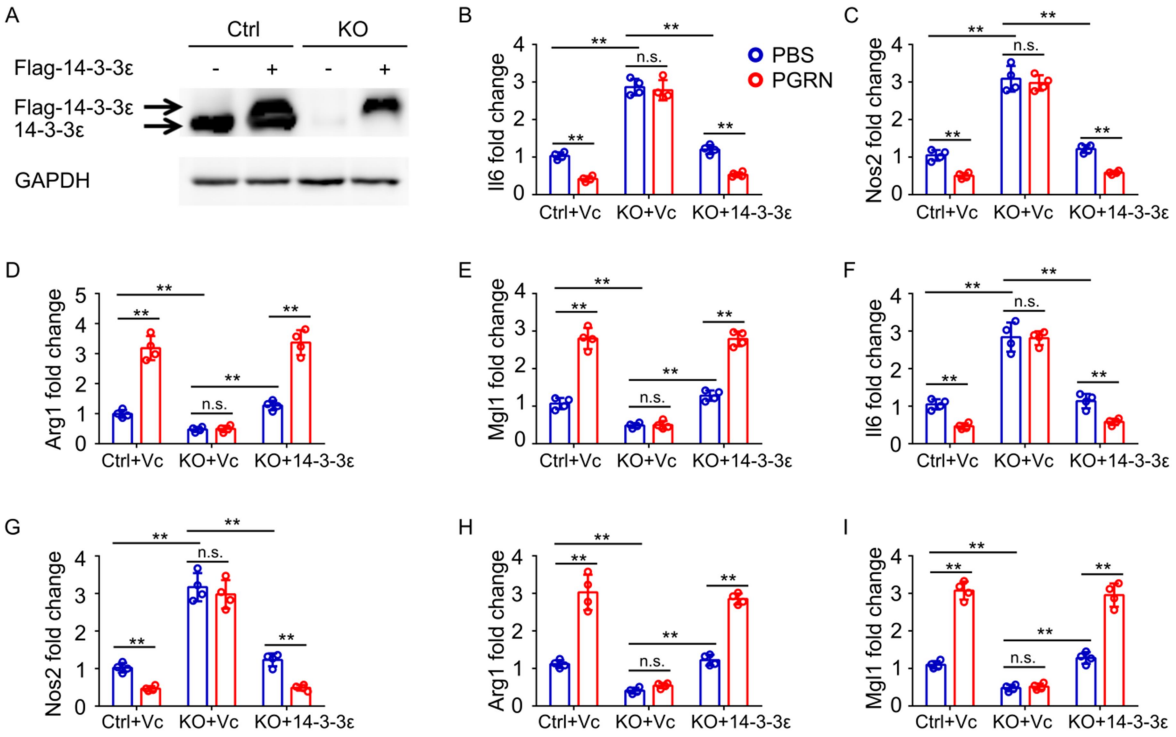

Fig. 3 14-3-3ε is required for TNFR2 signaling regulation of macrophage polarization. (**A**) Expression of Flag-14-3-3ε in 14-3-3ε-/- Raw264.7 cells. (**B-E**) Relative mRNA expression of *Il6* (**B**) and *Nos2* (**C**), or *Arg1* (**D**) and *Mgl1* (**E**) in control or 14-3-3ε-/- Raw264.7 cells with re-expression of 14-3-3ε which were polarized to M1 or M2 with or without 0.5μg/ml PGRN for 18h. (**F-I**) Expression of *Il6* (**F**) and *Nos2* (**G**), or *Arg1* (**H**) and *Mgl1* (**I**) in control or 14-3-3ε-/- Raw264.7 cells with re-expression of 14-3-3ε which were polarized from M2 to M1 or M1 to M2 with or without 0.5μg/ml PGRN for 18h, respectively. B-I, data are mean ± SD; n = 4 biological replicates; significant difference was analyzed by one-way ANOVA with post hoc Bonferroni test; $^{**}P < 0.01$. Vc, empty vector; Flag-14-3-3ε, pCMV-Flag-14-3-3ε plasmid.

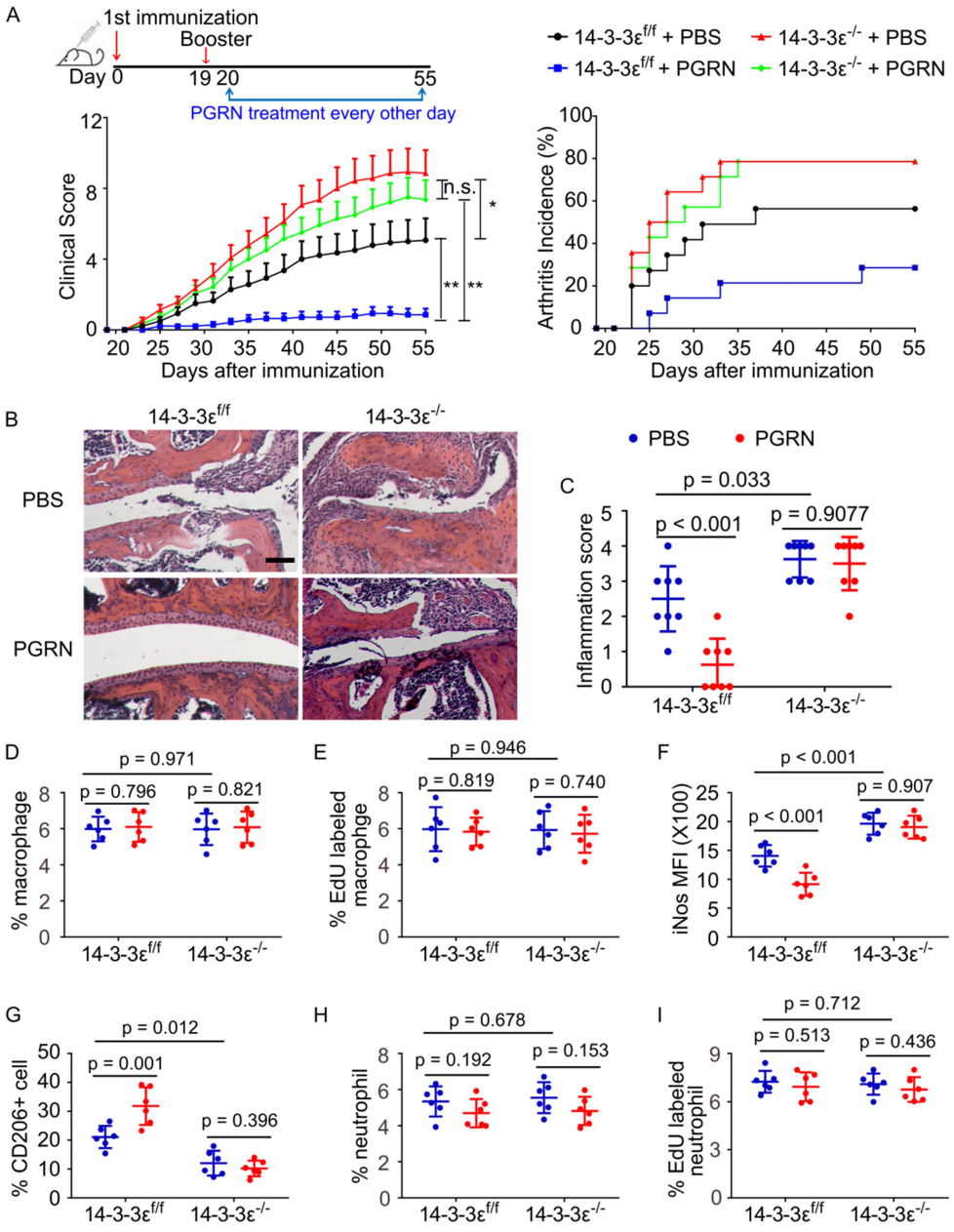

Fig. 4 Global knockout of 14-3-3ε renders B6 mice highly susceptible to collagen-induced arthritis (CIA). (**A**) Clinical arthritis scores and incidence of arthritis in the indicated mice with CIA. Data are mean ± SEM; n = 14 mice per group; significant difference was analyzed by one-way ANOVA with post hoc Bonferroni test. * P < 0.05 or * * P < 0.01. (**B, C**) Representative images of H&E staining, and quantification of histomorphometric analysis of synovial inflammation of ankle joints (n=8 mice per group). Scale bar, 100 μM. (**D-I**) The percentage of macrophages (D), Edu labeled macrophages in total macrophages (E), iNOS mean fluorescence intensity (MFI) of macrophages (F), percentage of CD206+ cells in CD11b+F4/80+cells (G), percentage of neutrophils (H) and percentage of EdU labeled neutrophils in total neutrophils (I) in the joints of indicated mice with CIA (n=6 mice for each group) were determined by flow cytometry. C-I, data are mean ± SD; significant difference was analyzed by one-way ANOVA with post hoc Bonferroni test.

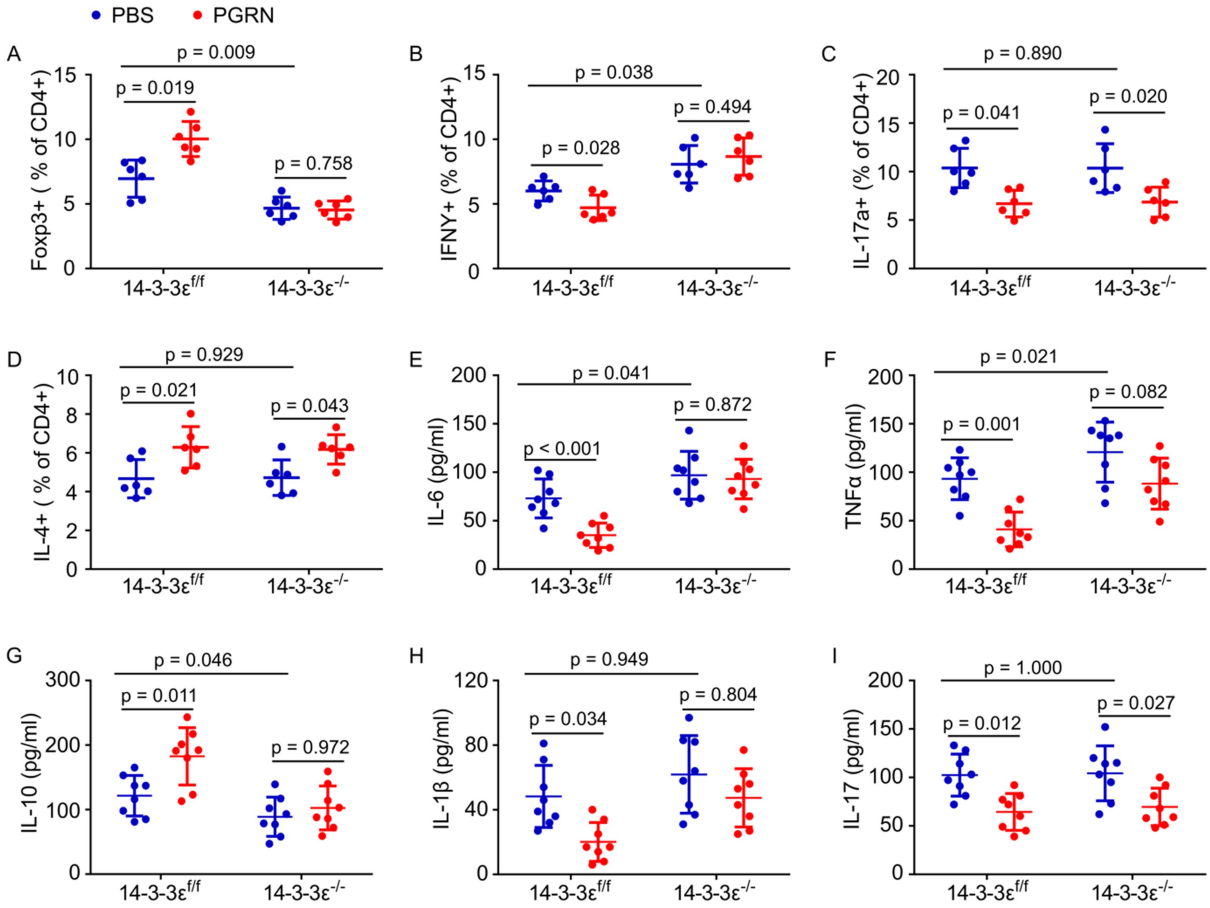

Fig. 5 14-3-3ε is implicated in mediating PGRN's regulations of T cells and inflammation in CIA. (**A-D**) Percentage of Treg (A), Th1 (B), Th17 (C), and Th2 (D) cells in CD4+ T cells in the joints of indicated mice with CIA (n=6 for each group) were determined by flow cytometry. (**E-I**) Serum levels of IL-6 (E), TNFα (F), IL-10 (G), IL-1β (H) and IL-17(I) in the indicated mice with CIA (n = 8 mice for each group), assayed by ELISA. Data are mean ± SD; significant difference was analyzed by one-way ANOVA with post hoc Bonferroni test.

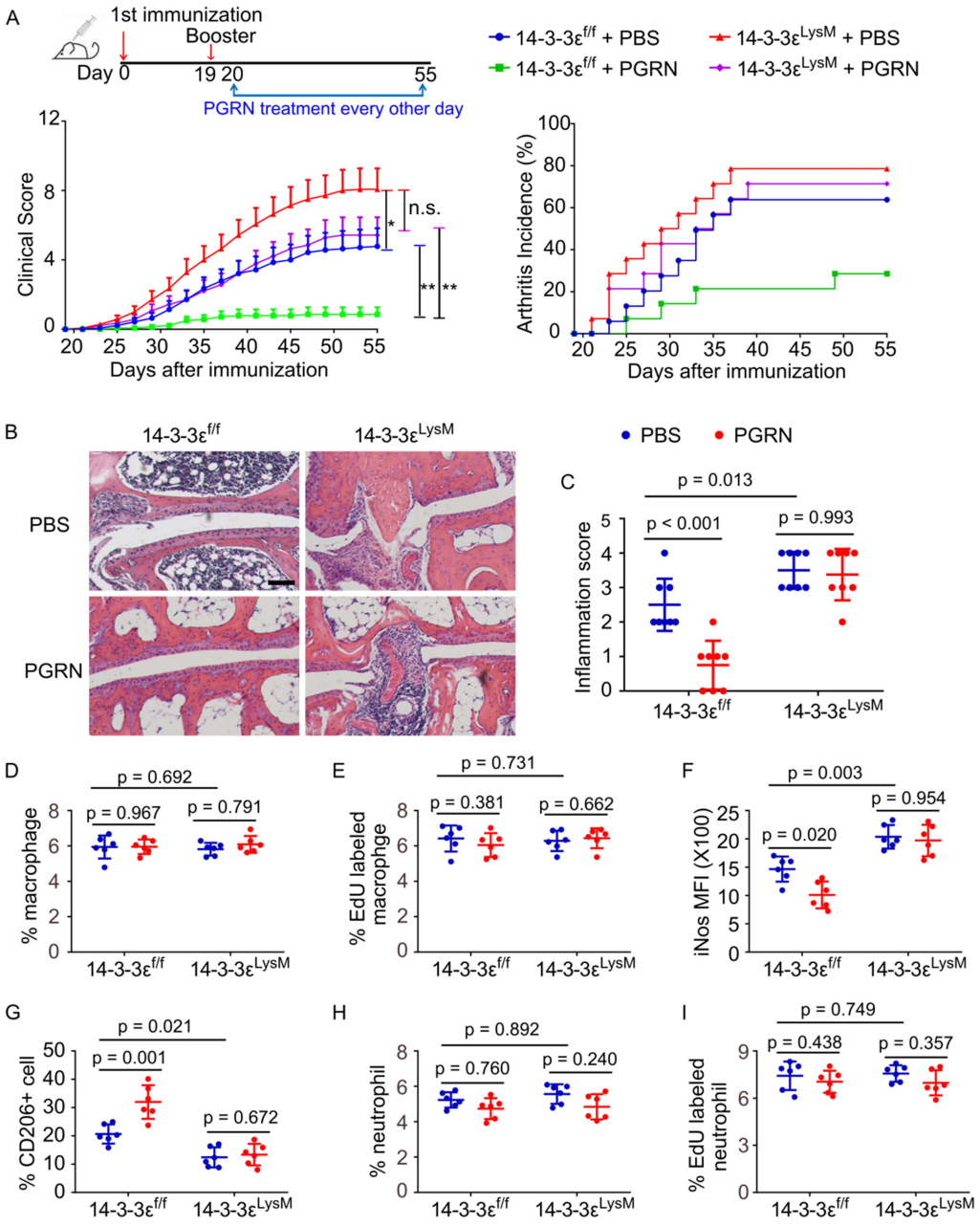

Fig. 6 Myeloid-specific deletion of 14-3-3ε worsens inflammation in collagen-induced arthritis (CIA). (**A**) Clinical arthritis scores and incidence of arthritis in the indicated mice with CIA. Data are mean ± SEM; n = 14 mice per group; significant difference was analyzed by one-way ANOVA with post hoc Bonferroni test. * P < 0.05 or * * P < 0.01. (**B, C**) Representative images of H&E and quantification of histomorphometric analysis of synovial inflammation of ankle joints. n = 8 mice per group. Scale bar, 100 μM. (**D-I**) The percentage of macrophages (D), Edu labeled macrophages in total macrophages (E), iNOS mean fluorescence intensity (MFI) of macrophages (F), percentage of CD206+ cells in CD11b+F4/80+ cells (G), percentage neutrophils (H), and EdU labeled neutrophils of total neutrophils (I) in the joints of indicated mice with CIA (n=6 for each group) were determined by flow cytometry. C-I, data are mean ± SD; significant difference was analyzed by one-way ANOVA with post hoc Bonferroni test.

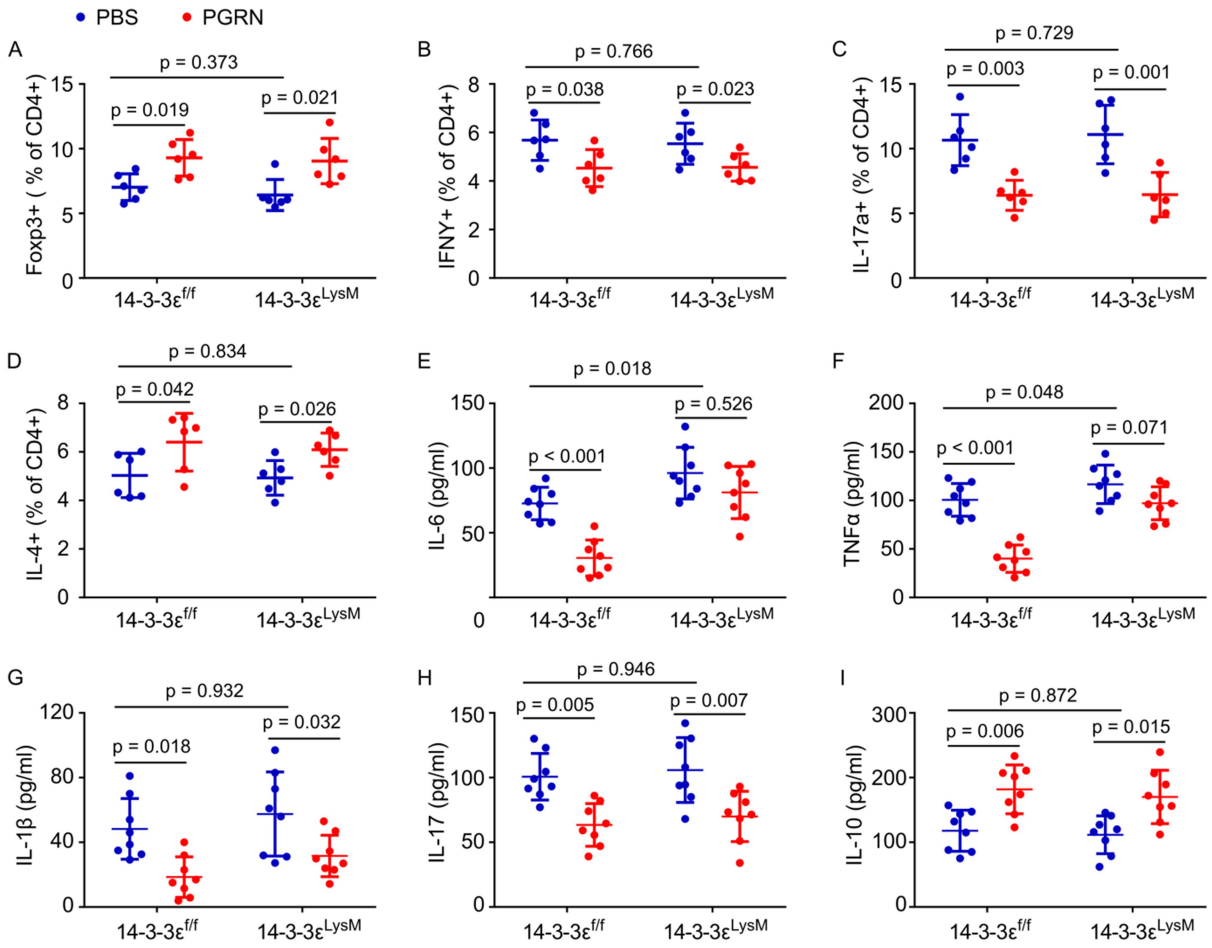

Fig. 7 14-3-3ε deficiency in myeloid lineage is implicated in PGRN regulation of serum levels of cytokines independent of T cells. (**A-D**) Percentage of Treg (A), Th1 (B), Th17 (C), and Th2 (D) cells in CD4+ T cells in the joints of indicated mice with CIA (n=6 for each group) were determined by flow cytometry. (**E-I**) Serum levels of IL-6 (E), TNFα (F), IL-1β (G), IL-17 (H), and IL-10 (I) in the indicated mice with CIA (n = 8 mice per group), assayed by ELISA. Data are mean ± SD; significant difference was analyzed by one-way ANOVA with post hoc Bonferroni test.

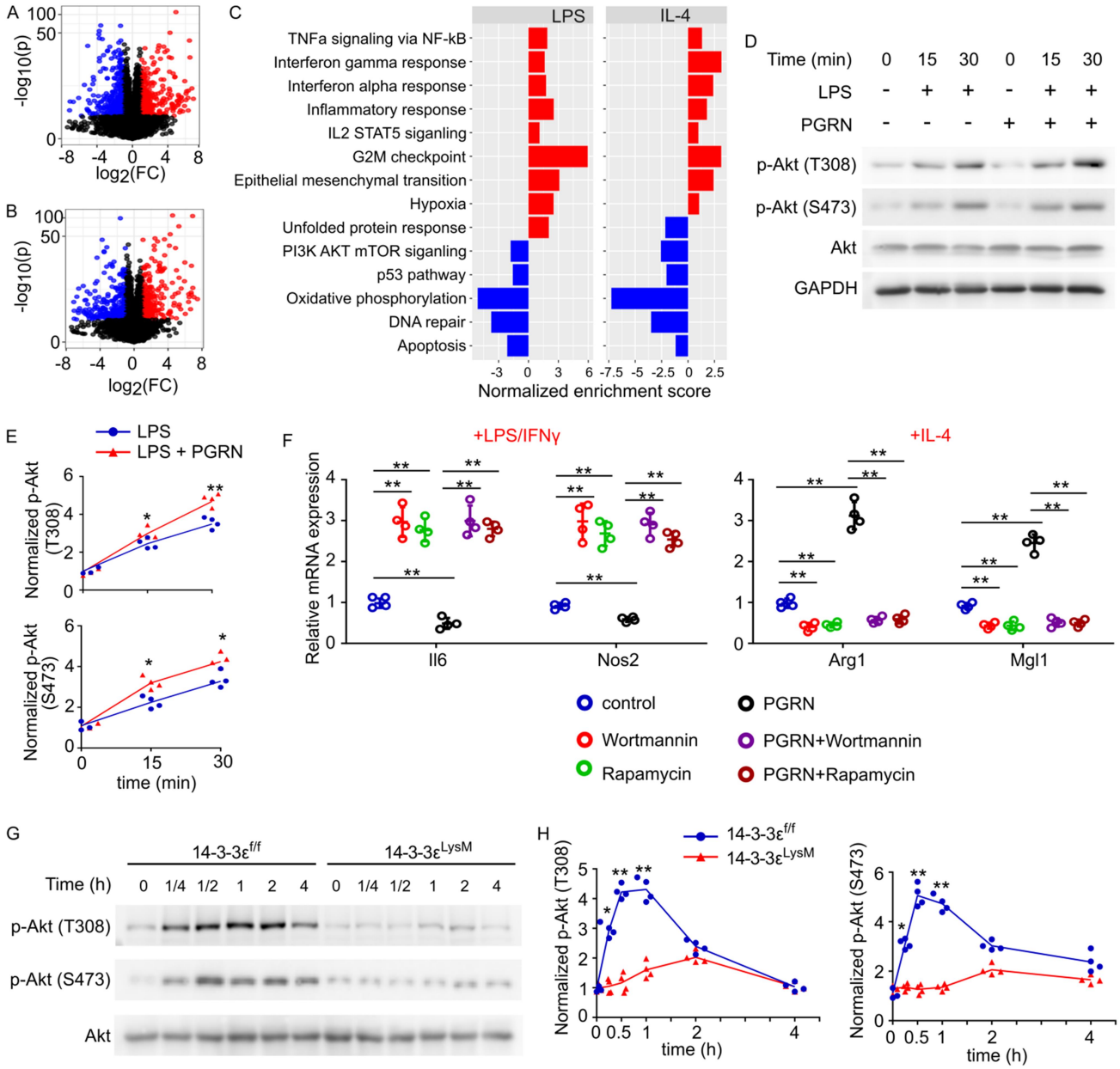

Fig. 8 PI3K/Akt/mTOR pathway is involved in 14-3-3ε regulation of macrophage polarization. (**A, B**) Volcano plots of differentially expressed transcripts in LPS/IFN-γ (A) or IL-4 (B) polarized 14-3-3ε$^{f/f}$ and 14-3-3ε^{LysM} macrophages obtained by RNA sequencing. n = 3 biological replicates. Linear models with empirical Bayes statistic (Limma) were used for differential expression. Genes in red or blue are up-regulated or down-regulated respectively in 14-3-3ε^{LysM} as compared to 14-3-3ε$^{f/f}$ macrophage with Benjamini–Hochberg adjusted $P < 0.05$. (**C**) Gene Set Enrichment Analysis (GSEA) analysis using hallmark gene sets from the Molecular Signature Database. The statistically significant signatures were filtered by gene sets with false discovery rates (FDR) < 0.25. Red bars represented the pathways up-regulated in the 14-3-3ε^{LysM} macrophages and blue bars indicated those enriched in 14-3-3ε$^{f/f}$ macrophage. (**D**) Immunoblotting of pAkt and Akt in LPS and PGRN stimulated WT BMDMs. GAPDH was used as the loading control. (**E**) Densitometry analysis of immunoblotting results shown in (D). (**F**) mRNA expression in PI3K- or mTOR inhibitor-treated BMDMs polarized to M1 (LPS/IFN-γ) or M2 (IL-4) in the presence or absence of 0.5 μg/ml PGRN. (**G**) Immunoblotting of pAkt and Akt in 14-3-3ε$^{f/f}$ 14-3-3ε^{LysM} BMDMs stimulated with LPS. GAPDH was used as the loading control. (**H**) Densitometry analysis of immunoblotting results shown in (g). D-H, data are mean ± SD; n = 4 biological replicates; significant difference was analyzed by one-way ANOVA with post hoc.

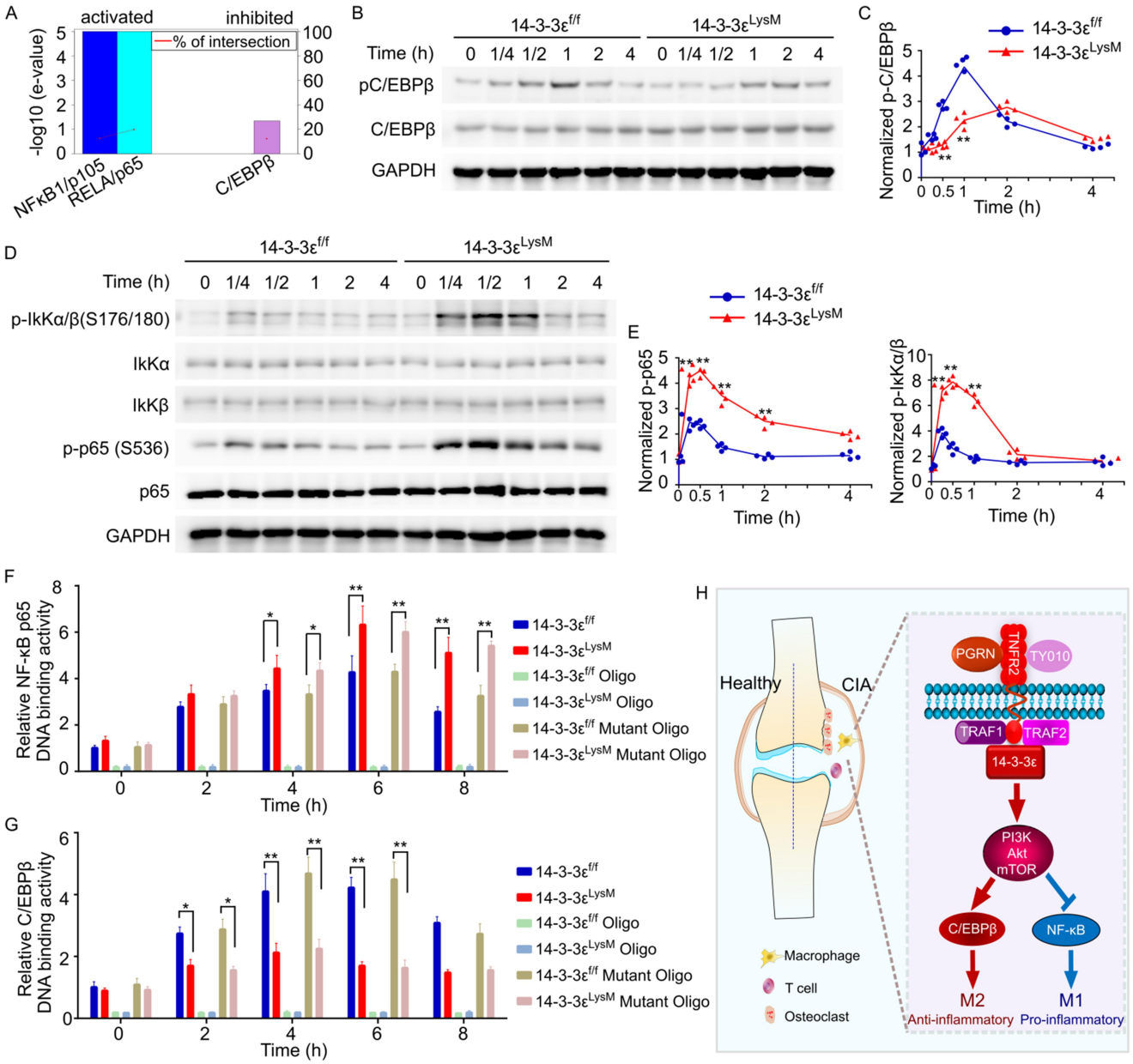

Fig. 9 14-3-3ε signals through NF-κB and C/EBPβ during macrophage polarization. (**A**) Transcription factors predicted to be activated or inhibited and are implicated in the differential regulation of inflammation in 14-3-3ε^{LysM} compared with 14-3-3ε$^{f/f}$ BMDMs by TFactS analysis. (**B**) Immunoblot analysis of selected signaling molecules in IL-4 stimulated 14-3-3ε$^{f/f}$ and 14-3-3ε^{LysM} macrophages. (**C**) Densitometry analysis of immunoblotting results shown in (B). (**D**) Immunoblot analysis of selected signaling molecules in LPS stimulated 14-3-3ε$^{f/f}$ and 14-3-3ε^{LysM} macrophages. (**E**) Densitometry analysis of immunoblotting results shown in (D). (**F, G**) NF-kB (F) and C/EBPβ (G) DNA binding activity in LPS and IL-4 stimulated 14-3-3ε$^{f/f}$ and 14-3-3ε^{LysM} macrophages. For competitive binding studies, functional (oligo) or nonfunctional (mutant oligo) oligonucleotides were used according to the manufacturer's instructions. C, E, F and G, data are mean ± SD; n = 4 biological replicates; significant difference was analyzed by unpaired Student's t-test (C, E) or one-way ANOVA with post hoc Bonferroni test (F, G); *$P < 0.05$ or **$P < 0.01$. (**H**) A proposed model depicting the signaling pathways by which PGRN/14-3-3ε/TNFR2 exerts anti-inflammation effects through regulating macrophage polarization.